Upper ocean carbon fluxes in the Atlantic Ocean: The importance of the POC:PIC ratio

Wolfgang Koeve

Marum, FB Geowissenschaften, Universität Bremen, Bremen, Germany

[1]   The mean depth distribution of the POC:PIC ratio of sinking particles, measured with particle interceptor traps deployed in the Atlantic Ocean, is fitted by an exponential function (POC:PIC = $64.3Z^{-0.56}$; $r^2 = 0.69$) The function is successfully evaluated by comparison with (a) estimates of the POC:PIC ratio of export production, computed from seasonal changes of nitrate and alkalinity and (b) estimates of the POC:PIC ratio of remineralization on shallow isopycnals. The basin mean POC:PIC ratio of export production is 4.2–4.37. The POC:PIC-depth function is combined with empirical relationships between the flux of particulate organic matter, primary production and depth, satellite derived primary production data sets, and the regional distribution of ψ (the ratio of released CO_2:precipitated carbonate during $CaCO_3$ formation) in order to estimate the effective carbon flux (J_{eff}) in the Atlantic Ocean. Remineralization of organic carbon above the winter mixed layer (11–17%) and $CaCO_3$ sequestration from the winter mixed layer (13–16%), which is the balance between $CaCO_3$ production and shallow dissolution, are the two main processes which control the difference between export production (0.9 and 2.9 GT C yr^{-1}) and J_{eff} (0.64 and 2.2 GT C yr^{-1}) on the basin scale (65°N to 65°S). $CaCO_3$ sequestration is the dominant process modulating effective carbon export in the tropics, while shallow POC remineralization dominates in temperate and polar waters. Observed regional patterns like polarward increases of the POC:PIC export ratio and of ψ counteract each other largely when J_{eff} is computed.   *INDEX TERMS:* 4203 Oceanography: General: Analytical modeling; 4806 Oceanography: Biological and Chemical: Carbon cycling; 4863 Oceanography: Biological and Chemical: Sedimentation; *KEYWORDS:* carbon cycle, particle flux, Corg:Cinorg ratio, effective carbon export, biological pump, Atlantic Ocean

Citation: Koeve, W., Upper ocean carbon fluxes in the Atlantic Ocean: The importance of the POC:PIC ratio, *Global Biogeochem. Cycles*, *16*(4), 1056, doi:10.1029/2001GB001836, 2002.

1.   Introduction

[2]   The biological pump [*Volk and Hoffert*, 1985] drives a net flux of fixed organic carbon from the surface of the ocean into its interior. This flux, and the subsequent remineralization in the deep ocean produces a vertical gradient of total CO_2, which controls the steady state CO_2 level of the atmosphere [*Shaffer*, 1993]. To determine the effectiveness of this carbon flux is at the heart of carbon cycle studies in the ocean [*SCOR*, 1990; *Fasham et al.*, 2001]. Export production [*Eppley and Peterson*, 1979], which is the sum of all organic carbon fluxes (particulate and dissolved organic carbon, POC and DOC) from the productive surface of the ocean, has often been referred to as a suitable measure of this effectivity. However, a significant fraction of the carbon export is remineralized within the upper few hundred meters [*Martin et al.*, 1987; *Louanchi and Najjar*, 2000] and nutrients and CO_2 stemming from

shallow remineralization can be recirculated to the surface ocean on short timescales of about a year and do not contribute to the vertical inner-ocean CO_2 gradient.

[3]   Additionally, a fraction of the organic carbon export is compensated by the export of particulate inorganic carbon (PIC, $CaCO_3$). This latter compensation is due to the net effect of $CaCO_3$ production and export on the surface ocean pCO_2. During formation of one mole of $CaCO_3$, alkalinity is reduced by two moles and total dissolved inorganic carbon decreases by one mole. In combination, these changes cause a shift in the carbonate system toward a higher CO_2-concentration and hence a higher pCO_2 [*Broecker and Peng*, 1982; *Robertson et al.*, 1994; *Frankignoulle et al.*, 1994; *Buitenhuis et al.*, 2001]. Like for organic carbon, sequestration of particulate inorganic carbon to the deep ocean is the balance between $CaCO_3$ production and shallow dissolution of $CaCO_3$. Hence, new carbon production, shallow remineralization of POC and the countereffective production, export and shallow dissolution of PIC must be considered to obtain a correct estimate of the carbon flux which is effective with respect to the steady state mean pCO_2 of the surface ocean.

[4] A useful measure of the effectivity of the biological pump is the net export of carbon, which reaches into water masses which are isolated from exchange with the atmosphere on decadal to centennial timescales, here referred to as J_{eff}. To estimate J_{eff} the export and the shallow remineralization and dissolution of POC and PIC need to be specified. However, we have a modest understanding of the large-scale patterns and integrals of these properties. Direct estimates of POC or PIC export from the euphotic zone, based on drifting particle interceptor traps [*Zeitzschel et al.*, 1978; *Asper*, 1996], are sporadic, short term in nature (days to weeks; *Martin et al.* [1993]), and methodologically questionable [*Gust et al.*, 1992; *Kähler and Bauerfeind*, 2001]. In particular, very few examples exist, which resolve the depth distribution of PIC fluxes in the upper ocean [*Martin et al.*, 1993]. Model-based estimates can fill some of these gaps. Ocean carbon cycle models have provided estimates of new production [*Najjar et al.*, 1992; *Sarmiento et al.*, 1993; *Six and Maier-Reimer*, 1996; *Oschlies et al.*, 2000], however, few such models [e.g., *Bacastow and Maier-Reimer*, 1990] included a formal description of the inorganic carbon cycle. Modeling of $CaCO_3$-related processes has usually restricted itself to dissolution at and below the lysocline in the deep ocean and in the sediments [*Archer*, 1991, 1996; *Sigman et al.*, 1998]. The production and fate of $CaCO_3$ in the upper ocean have rarely been studied quantitatively using ocean carbon cycle models [*Yamanaka and Tajika*, 1996; *Archer et al.*, 2000a]. Recently, one of these model studies [*Yamanaka and Tajika*, 1996] has challenged the paradigmatic idea that the POC:PIC ratio of the ocean is about $4-5$ [*Li et al.*, 1969; *Broecker and Peng*, 1982] and suggested values between 10 and 12.5. Solving this issue is of great importance for the understanding of suspected changes in the production of $CaCO_3$ [*Riebesell et al.*, 2000; *Zondervan et al.*, 2001] and their feedback on the future net CO_2-uptake of the ocean.

[5] Linking maps of primary production [e.g., *Berger*, 1989; *Longhurst et al.*, 1995; *Antoine and Morel*, 1996; *Antoine et al.*, 1996; *Behrenfeld and Falkowski*, 1997] with empirical relationships between particle flux (J), primary production (PP), and trap deployment depth (Z) [*Suess*, 1980; *Betzer et al.*, 1984; *Hargrave*, 1985; *Pace et al.*, 1987; *Berger et al.*, 1987 in the following referred to as *J*-PP-*Z* functions] provide an independent approach for basin scale estimates of POC fluxes in the ocean [*Antia et al.*, 2001]. These basin-scale POC flux estimates can be combined with empirical relationship of the POC:PIC flux ratio and water depth for the estimation of J_{eff} [*Antia et al.*, 2001].

[6] Recently *Antia et al.* [2001] and Koeve (W. Koeve, New production and shallow remineralization in the Atlantic Ocean–uncertainties and limitations of particle flux algorithms, submitted to *Journal of Marine Research*, 2001; in the following referred to as Koeve (submitted manuscript, 2001) estimated upper-ocean carbon fluxes for the Atlantic Ocean based on this empirical approach). A basin wide integrated carbon export production of 3.14 GT C yr^{-1} (equivalent to a mean *f*-ratio of 0.33) was estimated from a newly derived *J*-PP-*Z* function [*Antia et al.*, 2001]. POC fluxes were integrated over mixing cycles (i.e., from winter to winter) and corrected for trapping inefficiencies by

applying Th-calibration [*Scholten et al.*, 2001]. Remineralization above the winter mixed layer was about 5.7% of export production and compensation due to $CaCO_3$ export from the winter mixed layer reduced the carbon flux by another 16.5%. *Antia et al.* [2001] estimate the effective carbon export of the Atlantic Ocean to be 2.47 GT C yr^{-1}. Koeve (submitted manuscript, 2001), using a slightly different approach, showed estimates of export production to be very sensitive to the choice of the primary production forcing data set. Basin-scale means of export production (and the respective export ratio, ER) ranged between 0.9 and 2.9 GT C yr^{-1} (equivalent to an ER = $0.07-0.31$). The fraction of shallow remineralization was better constrained and showed a relationship with the depth of winter-time mixing, which for extratropical regions explained 92% of the variation of this fraction. Remineralization above the winter mixed layer depth was up to 62% of export production in the North Atlantic subarctic province.

[7] The overall aim of this paper is to describe the relative importance and the regional distribution of (a) shallow POC remineralization and (b) the $CaCO_3$ balance (production and shallow dissolution) for the adjustment of the effective carbon flux (section 4). For this purpose, the empirical relationship between flux ratios of organic to inorganic carbon (POC:PIC flux ratio; "rain ratio") from particle interceptor traps deployed in the Atlantic Ocean during the JGOFS decade [*SCOR*, 1990], and water depth is developed (section 3.1). This empirical relationship is evaluated by comparison with independent data. In particular, the POC:PIC export ratio (section 3.2), the vertical change of the POC:PIC ratio (section 3.4), and of the PIC flux (section 3.3) in the Atlantic are discussed during this comparison. In the following sections a short description of the data sets used and a definition of some fundamental terms are given.

2. Material and Methods
2.1. Data Sets, Depths Levels of Reference, Basin Scale Integration

[8] Three-dimensional data sets of the organic carbon flux in the Atlantic Ocean are adopted from the study of Koeve (submitted manuscript, 2001). In that study a suit of eight comparative data sets of particulate organic carbon fluxes in the ocean was computed from maps of primary production [*Antoine et al.*, 1996; *Behrenfeld and Falkowski*, 1997] and *J*-PP-*Z* flux functions. *J*-PP-*Z* fits were based on local estimates of primary production derived from the global primary production maps and Th^{230}-corrected [*Scholten et al.*, 2001] POC flux observations made in the Atlantic Ocean in the 1990s as part of the JGOFS program [*Antia et al.*, 2001]. A data set of POC:PIC flux ratios from particle flux studies in the Atlantic is also taken from the latter study. A detailed reference to the original particle flux data sets is given in the work by *Antia et al.* [2001] (their Table 1).

[9] This study focuses on carbon fluxes at two depth boundaries. Export production of particulate organic carbon ($JPOC_{exp}$) and particulate inorganic carbon ($JPIC_{exp}$) is the flux of POC and PIC across Z_{exp}. Operationally, and for the sake of easy comparison with published model results, Z_{exp} is defined as $Z = 125$ m in this study. The carbon flux into

Table 1. Empirical Relationships Between Flux Organic Particles (J), Primary Production (PP), and Trap Deployment Depths (Z)[a]

Data set	Method[b]	Parameter[c]			Regression Analysis[d]			n
		a	b	c	m	AA	r^2	
				J_c Versus J_i				
AM96	linear	1.69	−0.98	1.11	1.008	−0.005	0.410	24
BF97	linear	1.47	−0.92	0.82	1.010	0.001	0.428	24
				$ln(J_c)$ Versus $ln(J_i)$				
AM96	log	1.29	−0.99	7.69	0.993	−0.007	0.696	24
BF97	log	0.77	−1.00	62.2	0.998	0.002	0.696	24
				J_c Versus J_i				
AM96	linear	1.55	−0.72	0.30	0.992	0.008	0.791	23
BF97	linear	0.97	−0.74	3.00	0.993	0.005	0.790	23
				$ln(J_c)$ Versus $ln(J_i)$				
AM96	log	1.19	−0.89	5.47	1.003	−0.006	0.762	23
BF97	log	0.64	−0.92	63.4	1.007	0.006	0.756	23

[a] These empirical relationships are established for primary production [*Antoine et al.*, 1996; *Behrenfeld and Falkowski*, 1997] and particle flux [*Antia et al.*, 2001] data sets from the Atlantic ocean (from Koeve, (submitted manuscript, 2001); modified).
[b] Linear: linear optimization; log: logarithmic optimization.
[c] The parameters of the exponential function $J_c = cPP^a Z^b$ (equation (1)).
[d] Model II linear regression analysis of J_c versus J_i (linear optimization) or $ln(J_c)$ versus $ln(J_i)$ (logarithmic optimization); m = slope; AA = y-intercept; J_i are Th-corrected POC fluxes at depth Z_i; J_c are calculated POC fluxes (equation (1)) at depth Z_i and primary production PP_i; for details refer to the work of Koeve (submitted manuscript, 2001).

water masses which are isolated from exchange with the atmosphere on decadal to centennial timescales is referred to as *carbon sequestration*. It is distinguished between organic carbon sequestration ($JPOC_{sequ}$) and inorganic carbon sequestration ($JPIC_{sequ}$). The reference depth of carbon sequestration, Z_{sequ}, is estimated from the seasonal maximum depth of mixing (Z_{wml}). If, like in the tropics, Z_{wml} is shallower than 125 m, Z_{sequ} is set to 125 m. This is a rough approximation of the depth of the lower boundary of the equatorial undercurrent, which forms the source water mass for equatorial upwelling. The estimation of the annual maximum depth of mixing is based on monthly resolving climatologies of temperature and salinity (*NODC World Ocean Atlas*, 1994; *Monterey and Levitus*, 1997). The mixed layer depth is defined as the change in density with respect to the surface by 0.125 kg dm^{-3}. $JPOC_{exp}$, $JPIC_{exp}$, $JPOC_{sequ}$, and $JPIC_{sequ}$ are two-dimensional data sets with a resolution of 1° latitude × 1° longitude.

2.2. Formal Description of Carbon Fluxes

[10] Formally the depths dependence of the organic carbon flux J_{POC} can be empirically described according to equation (1).

[11] Sets of parameters a, b, and c (Table 1), which were determined for eight combinations of different PP- and particle flux data sets and fitting techniques, are taken from the study of Koeve (submitted manuscript, 2001). Empirical descriptions of PIC fluxes were not directly estimated from trap observations but by combining equation (1) with empirical fits of the POC:PIC flux ratio (RR) according to equation (2)

$$J_{POC} = cPP^a Z^b \qquad (1)$$

$$J_{PIC} = J_{POC}/RR \qquad (2)$$

[12] As will be discussed in the next section, RR can be described in various ways as a function of the trap deployment depth. For these empirical fits the full non-polar data set ($n = 76$) of *Antia et al.* [2001] is used. This data set combines observations ($n = 24$) for which the trapping efficiency has been estimated (Th^{230}-approach; *Scholten et al.* [2001]) and data sets for which no Th^{230} data were available. This procedure is justified by the observations that Th^{230} is not selectively trapped by organic or inorganic particles [*Scholten et al.*, 2001]. Estimating J_{PIC} according to equation (2) has the advantage that a larger and more representative data set can be used, however, at the expense of combining empirical relationships which are based on different data sets.

[13] J_{POC}, J_{PIC}, and RR are data sets on a three dimensional grid (latitude, longitude, depth). From J_{POC}, J_{PIC}, RR, and ψ, the ratio of *released CO_2:precipitated carbonate* during $CaCO_3$ precipitation [*Frankignoulle et al.*, 1994; see section 4.3.], a property called the net carbon flux, J_{net}, can be defined as the carbon export that drives a potential draw-down of CO_2 from the atmosphere to the ocean (equation (3)). J_{net} is defined on the same three dimensional grid as J_{POC}.

[14] Finally, J_{eff}, the effective carbon flux is defined as the value of J_{net} at $Z = Z_{sequ}$. This indicates that only the net flux of carbon across the sequestration depths, which is estimated from the annual maximum mixing depth (see section 2.1), is regarded as being really effective in driving a draw-down of CO_2 from the atmosphere to the ocean.

[15] Like $JPOC_{sequ}$ or $JPIC_{sequ}$, J_{eff} is a two dimensional data set on a latitude/longitude grid. In this study J_{eff} will be calculated according to equation (4), where $\overline{\Psi}$ indicates an appropriately averaged value of ψ (see section 4.3)

$$J_{net} = J_{POC} - \Psi J_{PIC} \qquad (3)$$

$$J_{eff} = JPOC_{sequ} - \overline{\Psi}JPIC_{sequ} \qquad (4)$$

Table 2. Abbreviations Used in This Study

Term	Units	Remarks
Z_{exp}	m	reference depth of export production, in this study Z_{exp} = 125 m
Z_{sequ}	m	reference depth of carbon sequestration (i.e., the export of carbon into water layers which do not exchange with the atmosphere on timescales of >1 yr)
Z_{wml}	m	climatological depth of the seasonal maximum of the mixed layer, winter mixed layer; in seasonal systems Z_{wml} is a good approximation of Z_{sequ}
$JPOC_{exp}$, $JPOC_{125}$	g C m^{-2} yr^{-1}	export production (also a measure of new carbon production); in this study $JPOC_{125}$, the flux of particulate organic carbon in 125 m depth is used as an approximation of $JPOC_{exp}$
$JPOC_{sequ}$	g C m^{-2} yr^{-1}	sequestration of organic carbon, i.e., the export of organic carbon across Z_{sequ}
$JPIC_{125}$	g C m^{-2} yr^{-1}	the export of particulate inorganic carbon across Z_{exp}
$JPIC_{sequ}$	g C m^{-2} yr^{-1}	the sequestration flux of particulate inorganic carbon across Z_{sequ}
J_{net}	g C m^{-2} yr^{-1}	net carbon flux, see equation (3); J_{net} is defined at any depth
J_{eff}	g C m^{-2} yr^{-1}	effective carbon flux, the flux of carbon which is effective with respect to the steady state surface pCO_2; J_{eff} is J_{net} across Z_{sequ}
Ψ	mol:mol	the ratio of released CO_2:precipitated $CaCO_3$ during calcium carbonate formation
$r_{R\text{-}POC_{sequ}}$	mol:mol	the fraction of export production of organic carbon, $JPOC_{125}$, which is remineralized above Z_{sequ}; $r_{R\text{-}POC_{sequ}}$ = ($JPOC_{125}$ − $JPOC_{sequ}$)/$JPOC_{125}$
$r_{R\text{-}PIC_{sequ}}$	mol:mol	the fraction of export of particulate inorganic carbon, $JPIC_{125}$, which is remineralized above Z_{sequ}; $r_{R\text{-}POC_{sequ}}$ = ($JPOC_{125}$ − $JPOC_{sequ}$)/$JPOC_{125}$
RR_{sequ}	mol:mol	the POC:PIC ratio ("rain ratio") at Z_{sequ}

[16] Abbreviations used in this study are summarized in Table 2.

3. POC:PIC Ratios

3.1. POC:PIC Flux Ratios From Particle Flux Observations

[17] Two functionalities of the vertical profile of the POC:PIC flux ratio (RR) are analyzed, a linear regression (model I) of RR over ln (Z) [Antia et al., 2001] (equation (5)) and an exponential fit (equation (6))

$$RR = d\,\ln(Z) + e \qquad (5)$$

$$RR = d\,Z^e \qquad (6)$$

[18] For the data from the Atlantic Ocean (Figure 1a) the best fits are RR = 0.827($\pm$0.0683)ln(Z) + 7.34 ($\pm$0.504)
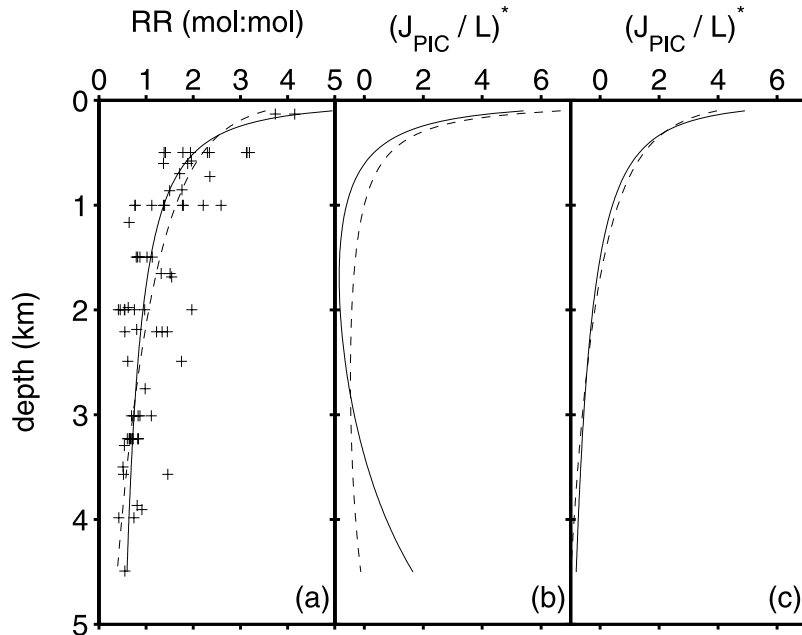

Figure 1. Vertical distribution of the POC:PIC flux ratio and PIC fluxes in the North Atlantic. (a) POC:PIC flux ratio (RR). +: observations, n = 76; *Antia et al.* [2001]. Solid line: exponential function, RR = 64.3 Z$^{-0.56}$; r^2 = 0.693 (this study). Dashed line: logarithmic fit, RR = 7.34 − 0.827 ln(Z); r^2 = 0.664 (this study). (b, c) Distribution of the normalized ((x_i-mean(x_i))/std(x_i)) and site independent relative vertical profile of J_{PIC}, named (J_{PIC}/L)*. Here L is a shortcut of the term cPP^a of equation (1) and b is the z-exponent of equation (1). (b) Estimates based on logarithmic RR-Z functions. Solid line: *Antia et al.* [2001]; b = −0.68, RR = 7.39 − 0.83 ln(Z); dashed line: this study; b = −1, RR = 7.34 − 0.827 ln(Z). (c) Estimates based on the exponential RR-Z function RR = 64.3Z$^{-0.56}$ from this study. Solid line: b = −1.0; dashed line: b = −0.7. Note the artificial increase in (J_{PIC}/L)* in the deep ocean in Figure 1b.

Table 3. Estimates of the POC:PIC Ratio of Production

Scenario	Latitude	$[NO_3/Si(OH)_4]$ (Winter)[a]	$f_{diatoms}$	POC:PIC Ratio of Production	Remarks
1	47°N	2.6	0.38	2.9	assuming a POC:PIC ratio of 6:1 during the diatom bloom[b]
2	47°N	2.6	0.38	4.0	like scenario 1, but assuming a POC:PIC ratio of 9:1 during the diatom bloom[c]
3	60°–62°N	2.0	0.5	3.5	assuming summer nitrate depletion and the POC:PIC ratio during the diatom bloom of 6:1
4	60°–62°N	2.0	0.64	4.2	assuming summer silicate depletion,[d] summer nitrate concentrations[e] of about 3 μmol dm^{-3}, and a contribution of coccolithophorids to post spring bloom new production of 100%
5	60°–62°N	2.0	0.64	5.1	assuming summer silicate depletion,[d] summer nitrate concentrations[e] of about 3 μmol dm^{-3}, and a contribution of coccolithophorids to post spring bloom new production of 50%
From Particle Flux Algorithms					
65°S–65°N				3.4	RR$_{125}$, RR-ln(Z)fit; from[f,g]
65°S–65°N				4.4	RR$_{125}$, exponential fit of RR; from[f]
From Seasonal Changes of CO_2, Alkalinity, and Nitrate					
NAST (27°–42°N)				3.9	province means of data presented in Figure 2; from[f]
NADR (42°–55°N)				4.3	-"-; from[f]
SARC/ARCT (>55°N)				6.1	-"-; from[f]
north of 40°N				5.3–5.9	from[h]
40°S–40°N				4.9–5.1	from[h]
				(4.2–4.4)	ratio in brackets is calculated for data without the warming period: whole year scaling factor used by[h]
south of 40°S				8.9–12.1	from[h]

[a] *Koeve* [2001].
[b] *Robertson et al.* [1994].
[c] *Takahashi et al.* [1990] as cited in the study by *Robertson et al.* [1994].
[d] *Veldhuis et al.* [1993].
[e] *Sambrotto et al.* [1993].
[f] This study.
[g] *Antia et al.* [2001].
[h] *Lee* [2001].

and RR = $64.3Z^{-0.56}$[ln(RR) = -0.557 (±0.0516)ln(Z) + ln(4.16 ± 0.381)], respectively. The statistics for both functions are quite similar. Model-II regressions [*Sokal and Rohlf*, 1995] of the predicted versus the observed flux ratios yield r^2 values of 0.664 (RR-ln Z) and 0.693 (exponential fit). A major difference, however, shows up, when JPIC is estimated from JPOC and the POC:PIC ratio according to equation (2). In the case of the RR-ln Z function JPIC decreases only down to about 1500 m but increases again in the deep ocean (Figure 1b). This unprecedented increase of the PIC flux is not seen if the POC:PIC ratio is estimated from the exponential fit. Here JPIC continuously decreases with depth (Figure 1c).

3.2. The POC:PIC Ratio of Export Production

[19] In this section the POC:PIC ratio of export production (RR$_{exp}$) is estimated based on the particle flux algorithms discussed above (section 3.2.1), an analysis of data from process studies in the North Atlantic (section 3.2.2), and finally, based on climatological data (section 3.2.3).

3.2.1. Estimates From Particle Flux Algorithms

[20] Using the exponential RR-Z function, a mean POC:PIC flux ratio in 125 m depth, RR$_{125}$, of 4.37 is estimated. Propagating the standard errors of the parameters d and e (see section 3.1) through the computation yields a range of 2.33–8.21 for RR$_{125}$. The logarithmic fit suggests an POC:PIC export ratio of 3.35 (±0.834).

3.2.2. Estimates From Field Studies in the North Atlantic

[21] Few local estimates of the POC:PIC ratio of production have been published to compare the estimates from the particle flux algorithm with. In the following I will combine estimates of the POC:PIC ratio of net carbon production during a coccolithophorid bloom in the subpolar North Atlantic and from spring bloom studies in the temperate and subpolar North Atlantic [*Robertson et al.*, 1994] with winter-time nutrient estimates [*Koeve*, 2001] to compute the range of the annually integrated POC:PIC ratio of new production in this region. *Robertson et al.* [1994] estimated the POC:PIC ratio from the relative change of potential alkalinity ($A_{pot} = A_t + NO_3$; *Fiadeiro* [1980]) and total CO_2 over time. They found POC:PIC ratios of production of 1:1 for a coccolithophorid bloom and 6:1 during a diatom spring bloom period. The annual mean POC:PIC ratio depends on the relative importance of diatoms, coccolithophorids, and non-calcifying flagellates (e.g., Phaeozystis) for annual new production. A first order estimate of the quantitative role of diatoms can be achieved from wintertime $NO_3:Si(OH)_4$ ratios and the mean nitrate:silicate uptake ratio of diatoms (about 1:1; *Richards*, 1958; *Brzezinski* [1985]). The decrease of wintertime $NO_3:Si(OH)_4$ ratios from 2.8 to 2 between 40°N and 60°N along 20°W [*Koeve*, 2001], converts to an increase of the relative contribution of diatoms to new carbon production from about 35–38% (at 40°N to 47°N) to 50–64% at 60°N ($f_{diatoms}$ in Table 3). How this ratio

translates to the annual POC:PIC ratio, depends on whether all post-diatom bloom nitrate is taken up over the growth season and which share coccolithophorids can take. If one assumes that all post-diatom bloom nitrate uptake is by coccolithophorids (with a POC:PIC ratio of 1:1, *Robertson et al.*, 1994), an annual POC:PIC ratio of net production between 2.9 and 4.0 is calculated for 47°N, and slightly higher values are found for 60°N (3.5–4.2) (Table 3).

[22] These are minimum estimates for the POC:PIC ratio of production, since new production by non-calcifying flagellates is ignored and since no correction for air sea exchange is taken into account. New production by non-calcifying phytoplankton after the diatom spring bloom will reduce the pool of nitrate and phosphate available for coccolithophorids and thereby increase the annual POC:PIC production ratio. Air-sea exchange, which was prominent (up to 25% of the apparent total CO_2 drawdown over 2–3 months) when the C:N ratios of new production was calculated from seasonal changes of total CO_2 and nitrate [*Körtzinger et al.*, 2001a], will act into the same direction. In particular, it will increase the POC:PIC ratio during the diatom spring bloom, since air-sea pCO_2 gradients and wind speed are higher during that season. Currently few process studies are available to describe the temporal and regional distribution of the POC:PIC export ratio in more detail. In the following section, I therefore present a first order estimate of the large scale distribution of the annual RR_{exp} in the Atlantic from a climatological perspective.

3.2.3. Large Scale Distribution of RR_{exp}

[23] In temperate and subarctic waters the surface mixed layer POC:PIC ratio of production (RR_{ML}) may be derived from the seasonal changes in salinity normalized total alkalinity and nitrate in the surface mixed layer and the C:N ratio of new production (equation (7)). Operationally it is assumed here that new carbon production (NP) which is exported via particles can be estimated from the seasonal drawdown of nitrate by multiplying with a constant C:N ratio of 6.625 [*Redfield et al.*, 1963; *Körtzinger et al.*, 2001a]. $CaCO_3$ production (P_{CaCO_3}) is estimated from seasonal changes of alkalinity and nitrate according to the concept of potential alkalinity (see section 3.2.2). In this section, however, data from climatologies of nitrate, alkalinity, and salinity are used to compute RR_{ML}. Details of the computation are given in Appendix A. It is assumed that the mixed layer POC:PIC ratio is an appropriate proxy of the export POC:PIC ratio RR_{exp} (i.e., $RR_{exp} \approx RR_{ML}$)

$$RR_{ML} = \frac{NP}{P_{CaCO_3}} = \frac{\Delta NO_3 \times C/N}{(\Delta A_t + \Delta NO_3)/2}$$
$$= \frac{\Delta NO_3}{(\Delta A_t + \Delta NO_3)} \times (C/N) \times 2 \quad (7)$$

[24] In the subtropics and tropics the seasonal approach cannot be used since seasonal gradients of alkalinity and nitrate vanish. As a substitute I estimate RR_{exp} from particle interceptor trap measurements [*Lohrenz et al.*, 1992] at the Bermuda Time Series Station (BATS). RR_{exp} at BATS is estimated to be 4.1–4.5 (see Appendix A for details).

[25] The major feature of the estimate of RR_{exp} in temperate and subarctic North Atlantic is a polarward gradient, overlaid by a weaker east-west gradient with maximal values in the North East Atlantic (Figure 2). Minima of RR_{exp} are seen at the boundary between the temperate and the subtropical domains (35°N and S) which is also the boundary between estimates from the seasonal change of potential alkalinity and estimates from shallow traps at BATS. The intensity of these minima is subject to the choice of the C:N ratio of sinking particles (see equation (7)) and the choice of the geographic position of the boundary itself. Province mean values of RR_{exp} in the temperate and subarctic North Atlantic increase northward from 3.9 (NAST) to 6.1 (SARC/ARCT) (Table 3), the weighted mean for the temperate and subarctic North Atlantic (all three provinces) is 4.37, which compares well with RR_{125} from the exponential RR-Z fit.

[26] Recently, *Lee* [2001] presented an analysis of the global net community production and the global $CaCO_3$ production based on an analysis of the annual cycle of surface water total CO_2 and alkalinity. They estimated organic carbon:inorganic carbon uptake ratios of 5.3–5.9 for the temperate and subarctic Atlantic (40°N–70°N), slightly lower values for the subtropical and tropical band (40°S–40°N: RR_{ML} = 4.9–5.1) but significantly higher values for the southern Ocean (Atlantic south of 40°S: RR_{ML} = 8.9–12.1). Their Atlantic integral value was 6.1–6.9. The estimate of net carbon production from seasonal changes in total CO_2 [*Lee*, 2001] does not differentiate whether carbon is stored and exported as particles or as DOC. One might use the difference between the RR_{ML} estimate from this study (4.2–4.37) and those from the study of *Lee* [2001] to approximate that on the mean 39–58% of net carbon production in the Atlantic is channeled through a seasonally accumulating pool of DOC [*Kähler and Koeve*, 2001] which eventually is exported from the mixed layer during winter time convection [*Carlson et al.*, 1994] but is respired above the winter mixed layer depth or on shallow isopycnals [*Doval and Hansell*, 2000] and hence does contribute little to carbon sequestration. Regarding the involved uncertainties (about ±30% for the estimates based on data from the work of *Lee*, 2001), both studies support that the organic:inorganic carbon ratio of export production in the Atlantic is close to the canonical value of about 4–5 [*Li et al.*, 1969; *Broecker and Peng*, 1982].

3.2.4. Polarward Increase of RR_{exp}

[27] Estimates from this study (sections 3.2.2 and 3.2.3) suggest a polarward increase of RR_{exp} in the Atlantic Ocean. This sounds counterintuitive since the subpolar North Atlantic, in particular waters south of Iceland, is well known for the frequent occurrence of coccolithophorid blooms [*Holligan and Balch*, 1991; *Holligan et al.*, 1993; *Fernandez et al.*, 1993; *Balch et al.*, 1996] and one might therefore expect the POC:PIC ratio of export production to be low.

[28] In section 3.2.2 (and Table 3) it was shown that the northward increase of RR_{exp} goes along with increases in the contribution of diatoms to annual new production, which were driven by a decrease of the winter NO_3:$Si(OH)_4$ ratio. Because of an overall deepening of the winter mixed layer from the subtropics to the subarctic North Atlantic winter time nutrient concentrations increase polarward [*Glover and Brewer*, 1988; *Koeve*, 2001]. Coccolithophorid blooms, i.e.,
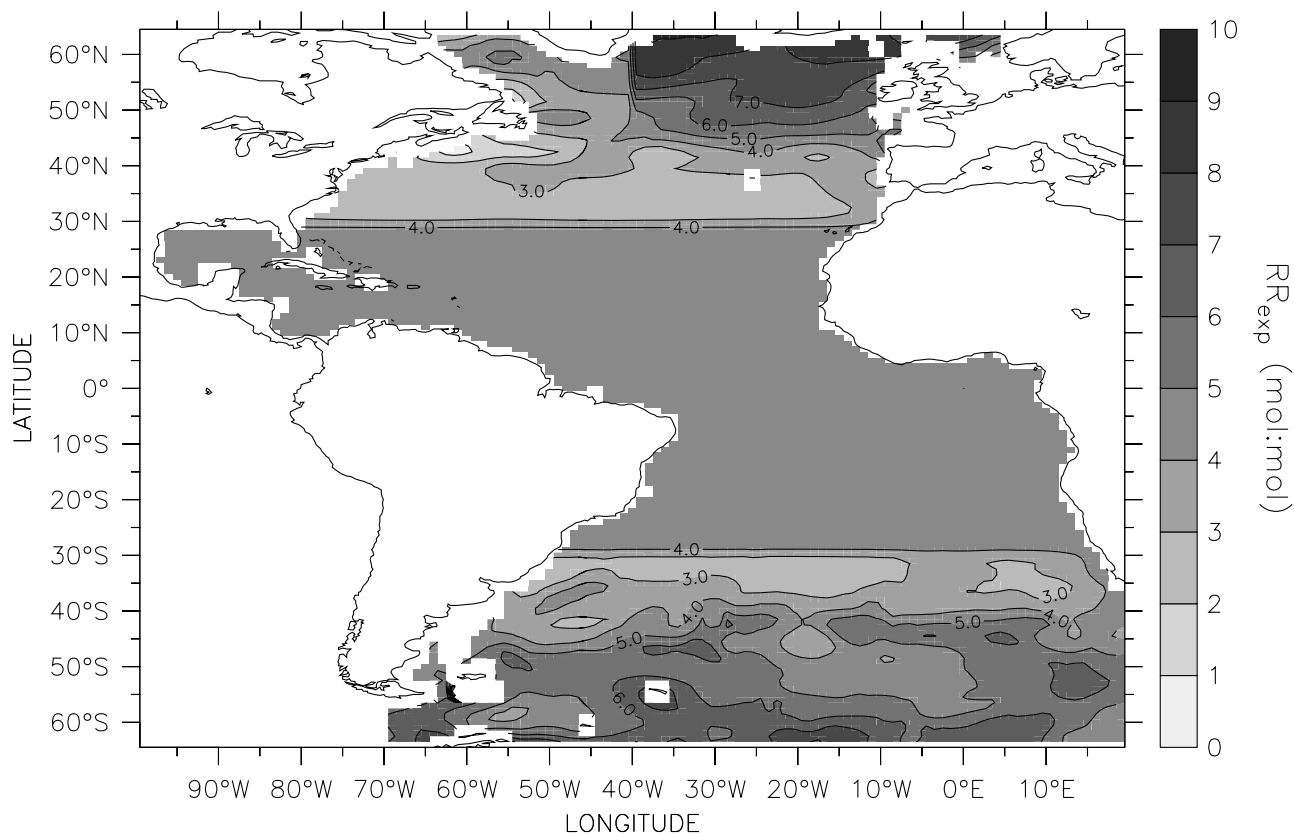
Figure 2. Regional distribution of RR_{exp} in the Atlantic Ocean. North of 35°N and south of 35°S, RR_{exp} is estimated from seasonal changes of potential alkalinity and nitrate. In the subtropical bands (10°–35°N, 10°–35°S) an estimate based on particle interceptor trap measurements at the Bermuda Time series Station (BATS) is assumed as a constant value. In the tropical band (10°S–10°N) an export flux ratio of 4.37 is used. For details see section 3.2.3 and the Appendix A.

high absolute rates of PIC production and the biomass of coccolithophorids, require high nitrate stocks after the diatom bloom has ended because of the depletion of silicate. Post-diatom bloom nitrate concentrations in the euphotic zone can be calculated to the first order from winter nitrate and silicate concentrations according to $NO_{3(post)} = NO_{3(winter)} - Si(OH)_{4(winter)} \times (N/Si)_{uptake\ ratio}$ (like in section 3.2.2. a mean $(N/Si)_{uptake\ ratio} = 1$ is assumed). Between 41°N and 59°N, the post-diatom bloom nitrate concentration increases from 2.9 to 6.5 mmol N m^{-3} at 59°N (calculated after data presented by *Koeve* [2001]). Simply by the availability of nitrate after the diatom bloom has ended there is an increasing potential for coccolithophorid blooms and $CaCO_3$ production toward the north. At the same time f_{diatom} (Table 3) and hence the POC:PIC production ratio increases northward. It is concluded, that the seemingly contradiction between increasing RR_{exp} toward the northern North Atlantic (this study) and observations of huge coccolithophorid blooms south of Iceland can be explained by the north-south distribution of relative and absolute rates at which nitrate and silicate are supplied to the surface ocean during winter mixing.

3.3. Evaluation of the Change of the PIC Flux Over Depth

[29] One of the oldest paradigms in oceanography states that pelagic $CaCO_3$ dissolves exclusively below the lyso-

cline and, due to high sinking speeds and slow dissolution, particularly within the sediments. Major evidence for this view is from the observation that vast areas and depth ranges of the ocean show a low corrosity for $CaCO_3$ (i.e., saturation state $\Omega > 0.8$), and from experimental studies of $CaCO_3$ dissolution [*Peterson*, 1966; *Keir*, 1980]. Along the same line, sediment trap data suggested that the PIC flux does not decrease significantly below 1000 m depth [*Tsunogai and Noriki*, 1991; *Milliman*, 1993]. This is accentuated in the North Atlantic [*Honjo*, 1990; *Honjo and Manganini*, 1993], where the depth of the calcite-lysocline is found at about 4000–4500 m.

[30] Combining the *J-PP-Z* functions of Koeve (submitted manuscript, 2001) (Table 1) and the POC:PIC ratio fits from this study allows to estimate changes in the PIC fluxes with depth. All parameter sets predict a significant decrease of the PIC flux in the upper 1000 m. The ratio of PIC fluxes in 125 and 1000 m, $JPIC_{125}/JPIC_{1000}$, varies between 1.4 and 2.5 (exponential RR fit; Figure 1c), indicating that 31–59% of the PIC export dissolves in the upper 1000 m. There are few data from (drifting) shallow sediment traps to compare this estimate with. The experiment of *Martin et al.* [1993] during the North Atlantic Bloom Experiment (NABE), in which floating VERTEX-type traps were deployed between 150 and 2000 m over the course of the spring bloom (6 weeks), supports a similar decrease in PIC fluxes of about

Table 4. Estimates of the POC:PIC Ratio of Remineralization

	Isopycnal	$\Delta O_2/\Delta Ca$[a]	$\Delta O_2/\Delta \Sigma CO_2$	RR_{remin}[b]	
North Atlantic	27.0	−11 ± 3	−1.3 ± 0.1	7.5 ± 3.0	$\Delta O_2/\Delta \Sigma CO_2$ from[c]
North Atlantic	27.2	−22 ± 7	−1.3 ± 0.1	16.0 ± 6.8	-"-
South Atlantic	27.0	−20 ± 5	−1.3 ± 0.1	14.4 ± 4.7	$\Delta O_2/\Delta \Sigma CO_2$ from[c]
South Atlantic	27.2	−24 ± 11	−1.3 ± 0.1	17.5 ± 9.4	-"-
Depth Range, m	**Isopycnal**	**Z-exponent of J-PP-Z Function (b)[d]**			
250–700	27.0	−0.7		8.3–14.7	for estimates based on the exponential fit of RR over Z from[e]
		−1.0		3.8–6.7	
450–1000	27.2	−0.7		6.8–10.6	-"-
		−1.0		3.1–4.8	
250–700	27.0	−0.7		1.2–2.1	for estimates based on the RR-lnZ fit; from[e]
		−1.0		1.4–2.4	
450–1000	27.2	−0.7		0.9–1.6	-"-
		−1.0		1.1–1.8	

[a] For $\Delta O_2/\Delta Ca$, the term ΔCa is estimated according to the concept of potential alkalinity from the change in total alkalinity (ΔTA) and the change in nitrate (ΔNO_3) according to $\Delta Ca = (\Delta TA + \Delta NO_3)/2$, *Takahashi et al.* [1985].
[b] $RR_{remin} = \Delta \Sigma CO_2/\Delta Ca - 1$.
[c] *Körtzinger et al.* [2001b].
[d] Koeve (submitted manuscript, 2001).
[e] This study.

50% in the upper 1000 m. *Milliman et al.* [1999] summarize the currently available evidence for shallow PIC dissolution and suggest that on average about 59% of the global carbonate production dissolves in the upper 1000 m.

[31] It is in this depth horizon where organic carbon fluxes change most rapidly; the ratio of the organic carbon fluxes at 125 and 1000 m, $JPOC_{125}/JPOC_{1000}$, varies between 4.5 and 8.1, suggesting an organic carbon remineralization of 77–88% within the upper 1000 m. A possible mechanism driving $CaCO_3$ dissolution above the lysocline is dissolution within "microenvironments" of high pCO_2, derived from intense remineralization of organic carbon. Here, the concentration of CO_3^{2-} could decrease locally such that the concentration product of CO_3^{2-} and Ca^{2+} becomes smaller than the dissolution product against the dissolution of $CaCO_3$. Such microenvironments might be either fecal pellets or aggregates of particulate organic matter. Organic aggregates [*Riley*, 1963; "marine snow"], which are a very important vehicle for the transport of biogenic matter into the deep ocean [*Fowler and Knauer*, 1986], are known as sites of active metabolism [*Pomeroy and Johannes*, 1968; *Turley*, 1992] and may be sites of shallow and microscale $CaCO_3$ dissolution. The build up of a pCO_2 (and CO_3^{2-}) gradient between the aggregate and the surrounding water would be a necessary prerequisite of a significant $CaCO_3$ dissolution in such aggregates. There is, however, conflicting evidence whether the degradation products (nutrients, CO_2, oxygen debt) accumulate in aggregates [*Brzezinski et al.*, 1997] or not [*Ploug and Joergensen*, 1999]. Another possible process to promote shallow PIC remineralization is dissolution in the guts of zooplankton [*Takahashi*, 1975]. Critical to this issue is, whether the pH of grazer guts is high [*Honjo and Roman*, 1978] or may, like in the case of starved copepods [*Pond et al.*, 1995], be low enough to support $CaCO_3$ dissolution. Recently, laboratory feeding experiments comparing the amount of ingested and egested coccolithophors, indicated dissolution rates of 50% and more [*Harris*, 1994]. *Milliman et al.* [1999] provide a detailed and thorough overview of the current evidence for and the processes involved in shallow $CaCO_3$ dissolution.

[32] Below 1000 m, PIC dissolution decreases with increasing depth (7.5–10.5% of $JPIC_{125}$ between 1000 and 2000 m, and 7–8% between 2000 and 4000 m). Overall, 46–77% of $JPIC_{125}$ dissolves above 4000 m depth. This is in good agreement with the finding of *Archer* [1996] and *Archer et al.* [2000a] that the global production rate of $CaCO_3$ required by the ocean surface/deep alkalinity contrast [*Li et al.*, 1969] is higher by roughly a factor of three than the average $CaCO_3$ rain rate to the seafloor required by sediment diagenesis models of *Archer* [1996], hence about 2/3 of calcium carbonate production dissolves in the water column.

3.4. POC:PIC Ratio of Remineralization

[33] In this section the organic carbon:inorganic carbon remineralization ratio (RR_{remin}) is estimated from the change of POC and PIC particle fluxes over depth, and from an analysis of the along-isopycnal change of the degradation products of POC remineralization and PIC dissolution in the interior of the ocean.

[34] In the latter case, RR_{remin} is calculated from $RR_{remin} = \Delta \Sigma CO_2/\Delta Ca - 1$ were Ca is computed from total alkalinity (TA) and nitrate, according to $Ca = (TA + NO_3)/2$. $\Delta \Sigma CO_2$ and ΔCa are estimated from regression slopes versus oxygen (ΔO_2) on isopycnals or neutral surfaces. I use $\Delta O_2/\Delta Ca$ ratios estimated by *Takahashi et al.* [1985] for shallow isopycnals just below the permanent thermocline (sigma-theta density levels $\sigma_\theta = 27.0$ and $\sigma_\theta = 27.2$; Table 4). *Takahashi et al.* [1985] report $\Delta O_2/\Delta \Sigma CO_2$ ratios, which range between -1.7 ± 0.1 and -2 ± 0.1. Their analysis, however, did not correct for the time history of the invasion of anthropogenic CO_2 into the ocean [*Takahashi et al.*, 1985]. The temporal change in anthropogenic CO_2 in the atmosphere causes a slight increase over time in the initial CO_2 concentration when a water mass is formed. If this effect is not taken into account, the $\Delta \Sigma CO_2$ due to remineralization along an isopycnal is underestimated and the $\Delta O_2/\Delta \Sigma CO_2$

ratio of remineralization is overestimated. Correcting for the time history of anthropogenic CO_2 invasion, *Körtzinger et al.* [2001b] estimate a $\Delta O_2/\Delta\Sigma CO_2$ ratio of -1.3 ± 0.1 for isopycnals just beneath the permanent thermocline. RR_{remin} on shallow isopycnals, thereafter, is estimated to range between $7.5-16.0$ (North Atlantic) and $14.4-17.5$ (South Atlantic) (see Table 4). These are mean estimates for the given ocean basins within which the specified isopycnals are encountered over a broad depth range of $250-700$ m ($\sigma_\theta = 27.0$) and $450-1000$ m ($\sigma_\theta = 27.2$).

[35] Within this depth range mean RR_{remin} estimated from particle flux data (exponential RR-Z relationship) range from 6.8 to 14.7 and 3.1 to 6.7 (Figure 3, thick lines) for values of the Z-exponent of the J-PP-Z function of $b = -0.7$ and $b = -1.0$, respectively. This range of b-values was found to be representative for the particle flux data set used in this study (Table 1). If the RR_{remin} estimate is based on the RR-ln Z relationship (Figure 3, thin lines) much lower values are estimated ($0.9-2.4$). Clearly RR_{remin} estimates from the exponential RR-Z relationship compare better with the RR_{remin} estimates from the isopycnal analysis than do those from the logarithmic RR-Z relationship. The difference between RR_{remin} estimates from the isopycnal analysis and from the exponential RR-Z particle flux relationship may be attributed to remineralization of DOC, which has been found to be significant on shallow isopycnals [*Doval and Hansell*, 2000].

3.5. POC:PIC Ratios: Some Conclusions

[36] Two alternative mathematical functions with almost identical statistics can be used to represent the mean depth dependence of the POC:PIC ratio of particle flux in the Atlantic ocean (section 3.1). However, only one of the models, the exponential function $RR = 64.3Z^{-0.56}$, yields (a) a consistent vertical distribution of the PIC flux (sections 3.1 and 3.3 and Figure 1c), (b) POC:PIC ratios of remineralization which match the distribution of breakdown products of POC remineralization and PIC dissolution on shallow isopycnals (section 3.4, Figure 3 and Table 4), and (c) POC:PIC export ratios (RR_{exp}) which agree with basin scale means of RR_{ML} estimates from seasonal changes of nutrients and alkalinity (section 3.2). On the contrary, the logarithmic RR-Z relationship which was adopted from the work of *Antia et al.* [2001] yields an unrealistic PIC increase in the deep ocean, too low POC:PIC ratios of remineralization, and also a too low mean POC:PIC export ratio.

4. Effective Carbon Flux

[37] The calculation of the effective carbon flux is based on three quantities, the sequestration fluxes of organic and inorganic carbon ($JPOC_{sequ}$, $JPIC_{sequ}$) and $\overline{\Psi}$, the integral ratio of released CO_2:precipitated carbonate (equation (4)). Two sets of J_{eff} calculations will be performed in section 4.4. In the first set one mean value for $\overline{\Psi}$ will be used together with estimates of $JPOC_{sequ}$ adopted from the study of Koeve (submitted manuscript, 2001) and $JPIC_{sequ}$ estimated after equation (2), applying the POC:PIC ratio estimates from the exponential RR-Z fit, i.e., with one, regionally invariable, vertical distribution of RR and a regionally constant value of RR_{exp}. In the second set a regionally variable data set of $\overline{\Psi}$
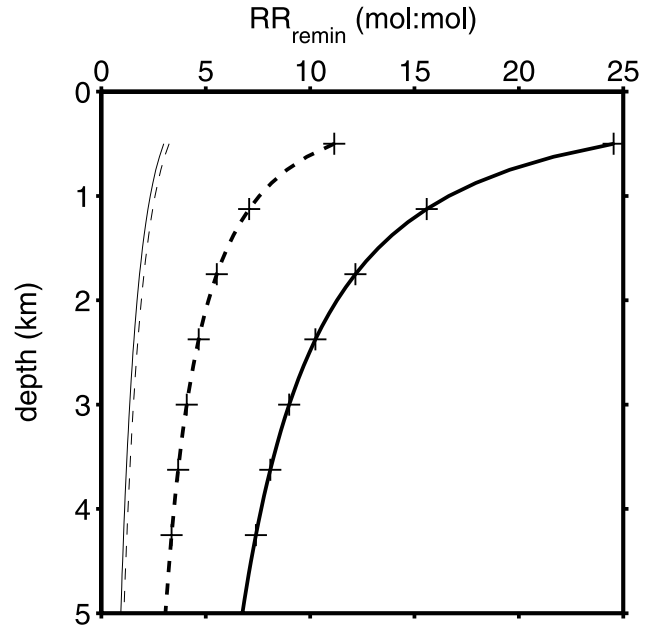

Figure 3. Vertical distribution of the POC:PIC ratio of remineralization. Thick solid line (with plus signs): exponential fit of RR-Z and $b = -0.7$, thick dashed line (with plus signs): exponential fit of RR-Z and $b = -1.0$. Thin solid line: logarithmic fit of the RR-Z function and $b = -0.7$, thin dashed line: logarithmic fit of the RR-Z function and $b = -1.0$; b is the z-exponent of equation (1).

(section 4.3) will be combined with a data set of $JPIC_{sequ}$ which is adjusted to the regional distribution of RR_{exp} discussed in section 3.2.3 and shown in Figure 2 and with the estimates of $JPOC_{sequ}$ from the work of Koeve (submitted manuscript, 2001). In the following three sections, I give a brief description of the distribution of $JPOC_{sequ}$ (section 4.1), $JPIC_{sequ}$ (section 4.2), and $\overline{\Psi}$ (section 4.3). In section 4.4 the resulting data fields of J_{eff} are discussed.

4.1. Distribution of $JPOC_{sequ}$

[38] The distribution of organic carbon fluxes in the Atlantic is discussed in detail in the study of Koeve (submitted manuscript, 2001) and is described here only in brief. Basin scale ($65°N-65°S$) integrals of export production computed from eight independent parameter fits (Table 1) of equation (1) varied between 0.9 and 2.9 GT C yr^{-1} (Table 5); the respective ER_{125} ($JPOC_{125}/PP$), which is an estimate of the f-ratio, ranged from 0.07 to 0.31. Not only overall fluxes and ratios differ, but also their N-S distribution patterns and the relative importance of tropical versus "spring-bloom" biogeographical provinces (Figure 4a). The regional distribution of export production and ER_{125} was in particular sensitive to the choice of the primary production input data set (data presented by *Antoine et al.* [1996] versus data presented by *Behrenfeld and Falkowski* [1997]). The percent fraction of carbon remineralized within the winter mixed layer (Figure 4b) could be estimated more robustly. For the Atlantic Ocean as a whole remineralization within the winter mixed layer reduces the carbon export by $11-17\%$ (Table 5). In the temperate and subpolar provinces of the North Atlantic, this

Table 5. Basin Wide Integrals for the North Atlantic[a]

	AM96-Based,[b] Means ± s.d.	BF97-Based,[c] Means ± s.d.	Minimum Estimate	Maximum Estimate
Primary production[d,e]	9.64	12.88		
Export production[d,e]	2.17 ± 0.722	1.47 ± 0.416	0.92	2.95
Remineralization[d,e]	0.26 ± 0.091	0.25 ± 0.084	0.14	0.35
$JPOC_{sequ}$[d,e]	1.91 ± 0.631	1.21 ± 0.333	0.77	2.60
$\psi JPIC_{sequ}$[d,f]	0.32 ± 0.102	0.21 ± 0.056	0.14	0.43
J_{eff}[d,f]	1.60 ± 0.529	1.00 ± 0.277	0.64	2.18
Respiration ratio,[e] $r_{R-POC_{sequ}} = (JPOC_{125} - JPOC_{sequ})/JPOC_{125}$	0.12 ± 0.006	0.16 ± 0.012	0.11	0.17
$CaCO_3$ compensation ratio,[f] $r_{CaCO_3} = \psi \times JPIC_{sequ}/JPOC_{125}$	0.15 ± 0.002	0.14 ± 0.003	0.14	0.15
r_{CaCO_3}[g]	0.15 ± 0.002	0.16 ± 0.003	0.15	0.16
r_{CaCO_3}[h]	0.15 ± 0.003	0.15 ± 0.004	0.15	0.16
r_{CaCO_3}[i]	0.14 ± 0.004	0.14 ± 0.004	0.13	0.14

[a] Estimates are presented for the Atlantic Ocean between 65°N and 65°S; marginal seas like the Baltic, the Hudson Bay, and the Mediterranean are excluded. The integration is based on a 1° × 1° data set, grid points where the seasonal maximum of the mixed layer depth is equal or larger than the mean water depth at the grid point are ignored.

[b] AM96-based estimates use the primary production data set of *Antoine et al.* [1996].

[c] BF97 based estimates use the primary production data set of *Behrenfeld and Falkowski* [1997].

[d] All in GT POC-C-equiv. yr^{-1}; ratios ($r_{R-POC_{sequ}}$; r_{CaCO_3}) are all in mol:mol.

[e] From Koeve (submitted manuscript, 2001).

[f] For the standard case: $\psi = 0.67$; $RR_{exp} = 4.37$.

[g] With ψ from Figure 6a, RR_{exp} from Figure 2.

[h] With ψ from Figure 6b, RR_{exp} from Figure 2.

[i] With ψ from Figure 6b, RR_{exp} as in the standard case.

reduction is equivalent to 37–61% of the export production. The sequestration of organic carbon, $JPOC_{sequ}$ was estimated to range between 0.77 and 2.6 GT C yr^{-1} (Table 5), the regional distribution of the province means of $JPOC_{sequ}$ is shown in Figure 4c.

4.2. Distribution of $JPIC_{sequ}$

[39] The distribution of the PIC export ($JPIC_{125}$, Figure 5a) is basically a scaled plot of the export production, if the POC:PIC flux ratio (RR) is estimated as a function of depth only and $RR_{exp} = RR_{125} = $ constant $= 4.37$. The estimate of the Atlantic wide integral of $JPIC_{125}$ ranges from 0.21 to 0.68 GT C yr^{-1}, PIC dissolution within the winter mixed layer, as predicted from the change of RR over depth, accounts for 0.011–0.047 GT C yr^{-1} or 4.6–9.4% of the export PIC flux. The north-south distribution of the ratio $r_{R-PICsequ}$ (=$Remin_{PICsequ}/JPIC_{125}$) (Figure 5b) is similar to the distribution of the fraction of POC remineralization to POC export production, $r_{R-PICsequ}$ (Figure 4b), however, the absolute values of $r_{R-PICsequ}$ are always smaller than $r_{R-PICsequ}$ $JPIC_{sequ}$ differs from $JPIC_{125}$ mainly in the North Atlantic (Figure 5a, c).

[40] Consequently the POC:PIC flux ratio of carbon sequestration ($RR_{sequ} = JPOC_{sequ}/JPIC_{sequ}$) decreases where the difference between POC remineralization and PIC dissolution can take effect, i.e., in the deep mixing regions of the North Atlantic (Figure 5d). North of 42°N (NADR, SARC/ARCT) RR_{sequ} is reduced by about 24–40% compared to the initial value of RR_{125}. Since tropical and subtropical regions, which are characterized by low values of $r_{R-PICsequ}$, dominate by area, the overall effect of this reduction on the Atlantic wide mean value of RR ($\overline{RR_{sequ}} \approx 3.9$) is small.

4.3. Released CO_2: Precipitated Carbonate Ratio, ψ
4.3.1. Mean ψ

[41] The ratio of released CO_2:precipitated carbonate during $CaCO_3$ formation, ψ, is controlled by carbonate

system chemistry and shows a weak relationship with salinity, a negative correlation with temperature, and a positive correlation with pCO_2 [*Frankignoulle et al.*, 1994]. The value of ψ in the surface ocean will mainly vary together with temperature and pCO_2. For the early 1990s, the time period of sediment trap deployments used in this study, an integral value for $\overline{\Psi} = 0.67$ can be estimated. This value assumes a mean ocean equilibration temperature of about 15°C [*Archer et al.*, 2000b], $S = 35$, and a mean surface ocean pCO_2 value of 350 μatm, and is estimated by interpolation of data presented in the study by *Frankignoulle et al.* [1994] (their Figure 2). This is a more realistic mean value than $\overline{\Psi} = 0.6$, which was applied by *Antia et al.* [2001], since that value requires the mean temperature of the ocean to be 25°C, for $S = 35$ and $pCO_2 = 350$ μatm [*Ware et al.*, 1992].

4.3.2. Regional Distribution of ψ in the Atlantic Ocean

[42] In the following an estimate of the regional distribution of ψ in the Atlantic is provided. Since these estimates of ψ will be used to compute annual fluxes of J_{eff}, they need to integrate in a suitable way over the depth range between the surface and Z_{sequ} and over the annual mixing cycle. Accordingly, I have chosen to estimate ψ based on the local mean temperature of the mixed layer at the time of deepest mixing (i.e., during winter). $CaCO_3$ production might take place under conditions of significantly warmer temperatures during summer (i.e., with a smaller ψ). However, the net effect on the steady state surface ocean pCO_2 is fixed at the end of winter time mixing when surface waters, which were "impoverished" in CO_2 due to CO_2-uptake during new production, have mixed with subsurface waters, which were enriched in CO_2 due to remineralization of organic carbon, and high wind speeds have brought the surface ocean, which during this season is characterized by low biological activity and low biogenic CO_2 fluxes, as close as possible to equilibrium with the atmosphere. A first estimate (ψ_{350}, Figure 6a) is based on the assumption that the surface pCO_2
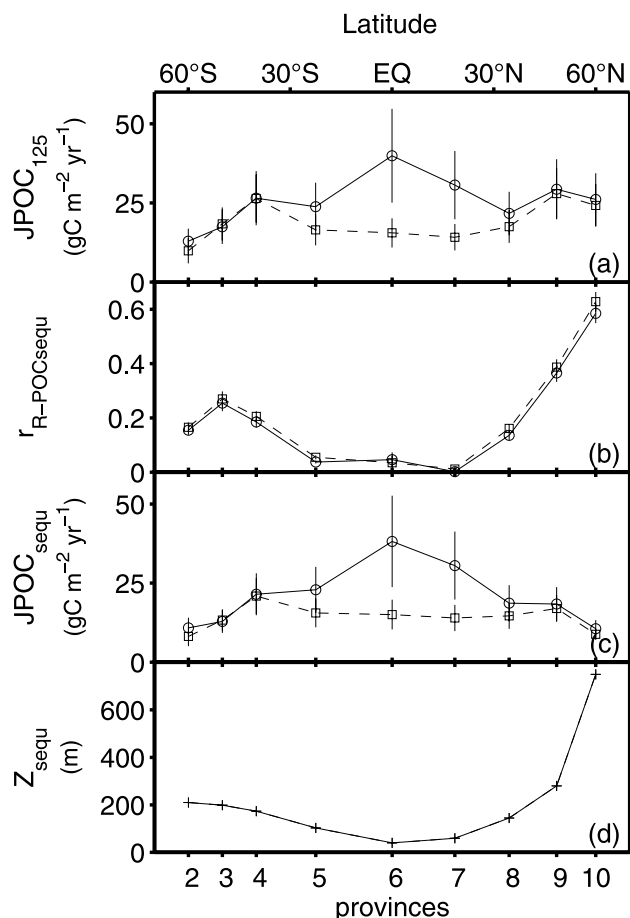
Figure 4. North-South distribution of organic carbon export. Meridional integrals of characteristic open ocean biogeographical provinces, basically following the schema suggested by *Longhurst* [1998], are presented. Province definitions used in this study are as follows (numbers are as indicated on the lower *x*-axes): (2) Atlantic sectors of the Antarctic Province (ANTA; 65°S–55°S, 70°W–20°E), (3) Subantarctic Water Ring Province (SANT; 55°S–45°S, 70°W–20°E), (4) South Subtropical Convergence Province (SSTC; 45°S–35°S, 70°W–20°E), (5) South Atlantic Gyral Province (SATL; 35°S–10°S), (6) Western and Eastern Tropical Atlantic Province (WETRA; 10°S–10°N), (7) North Atlantic Tropical Gyral Province (NATR, 10°N–27°N, including the Caribbean Province), (8) North Atlantic Subtropical Gyral Province (NAST, 27°N–42°N, including the Gulf Stream Province), (9) North Atlantic Drift Region (NADR; 42°N–55°N), and (10) the combined Atlantic Subarctic and Arctic Provinces (SARC and ARCT; 55°N–65°N). The following properties are shown: (a) province means of the export production $JPOC_{125}$ (g C m^{-2}yr^{-1}); (b) $r_{R\text{-}POCsequ}$, the fraction of POC-remineralization above the winter mixed layer ($RPOC_{sequ}$): export production ($JPOC_{125}$); (c) province means of $JPOC_{sequ}$, the sequestration flux of organic carbon, (g C m^{-2}yr^{-1}); (d) the province mean of Z_{sequ} (m). Solid lines/circles: means ($\pm$ standard deviation) of estimates based on primary production forcing data from the study of *Antoine et al.* [1996], dashed lines/squares: *Behrenfeld and Falkowski* [1997] based estimates. Modified after the work by Koeve (submitted manuscript, 2001).

is in equilibrium with the atmosphere (pCO_{2atm} = 350 µatm). ψ_{350} increases from low values (0.56–0.6) in the tropics to 0.7–0.82 in high latitudes. A second estimate of the distribution of ψ, in this case corrected for the deviation of the winter time surface pCO_2 from equilibrium with the atmosphere ψ_{pCO_2} insitu is given in Figure 6b. Both estimates agree within $\pm$0.02 mol:mol north of about 40°S. It is concluded that the specific effect of $CaCO_3$ sequestration on J_{eff} is sensitive to whether $CaCO_3$ is formed in cold or in warm (high- or low-latitude) waters. As I shall discuss in the next section in more detail, the polarward increase of ψ tends to counteract the polarward increase of the POC:PIC export ratio discussed in sections 3.2.2 and 3.2.3.
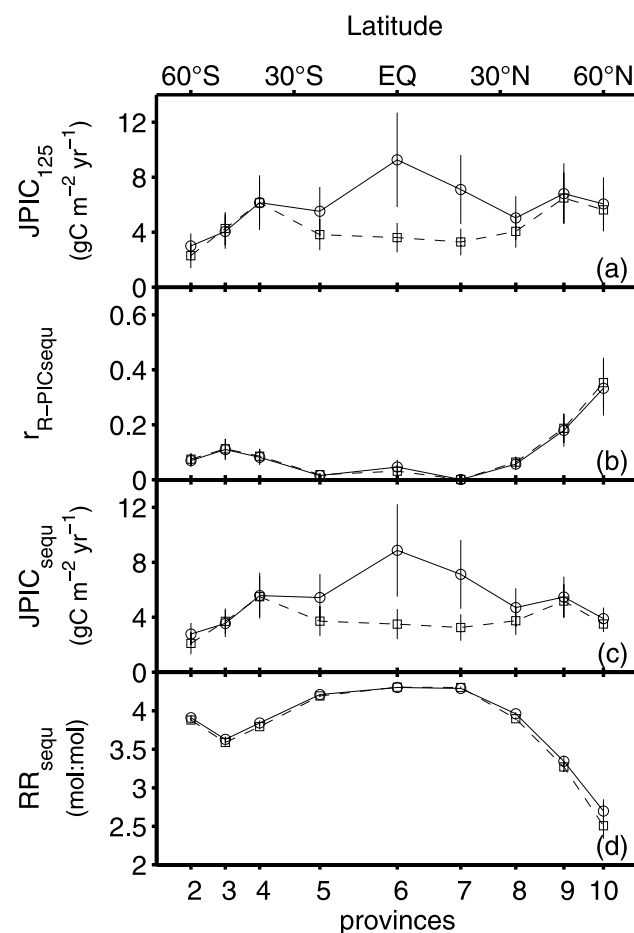

Figure 5. North-south distribution of particulate inorganic carbon fluxes in the Atlantic Ocean. The following properties are shown: (a) province means of the PIC export ($JPIC_{125}$, g C m^{-2}yr^{-1}), (b) the fraction of PIC dissolution above the winter mixed layer depth, (c) province means of the PIC-sequestration flux ($JPIC_{sequ}$, g C m^{-2} yr^{-1}), and (d) RR_{sequ}, the POC:PIC flux ratio at Z_{sequ}. For details see text. Solid lines/circles: estimates based on primary production forcing data from the study of *Antoine et al.* [1996], dashed lines/squares: estimates based on the work of *Behrenfeld and Falkowski* [1997]. For province captions see Figure 4.
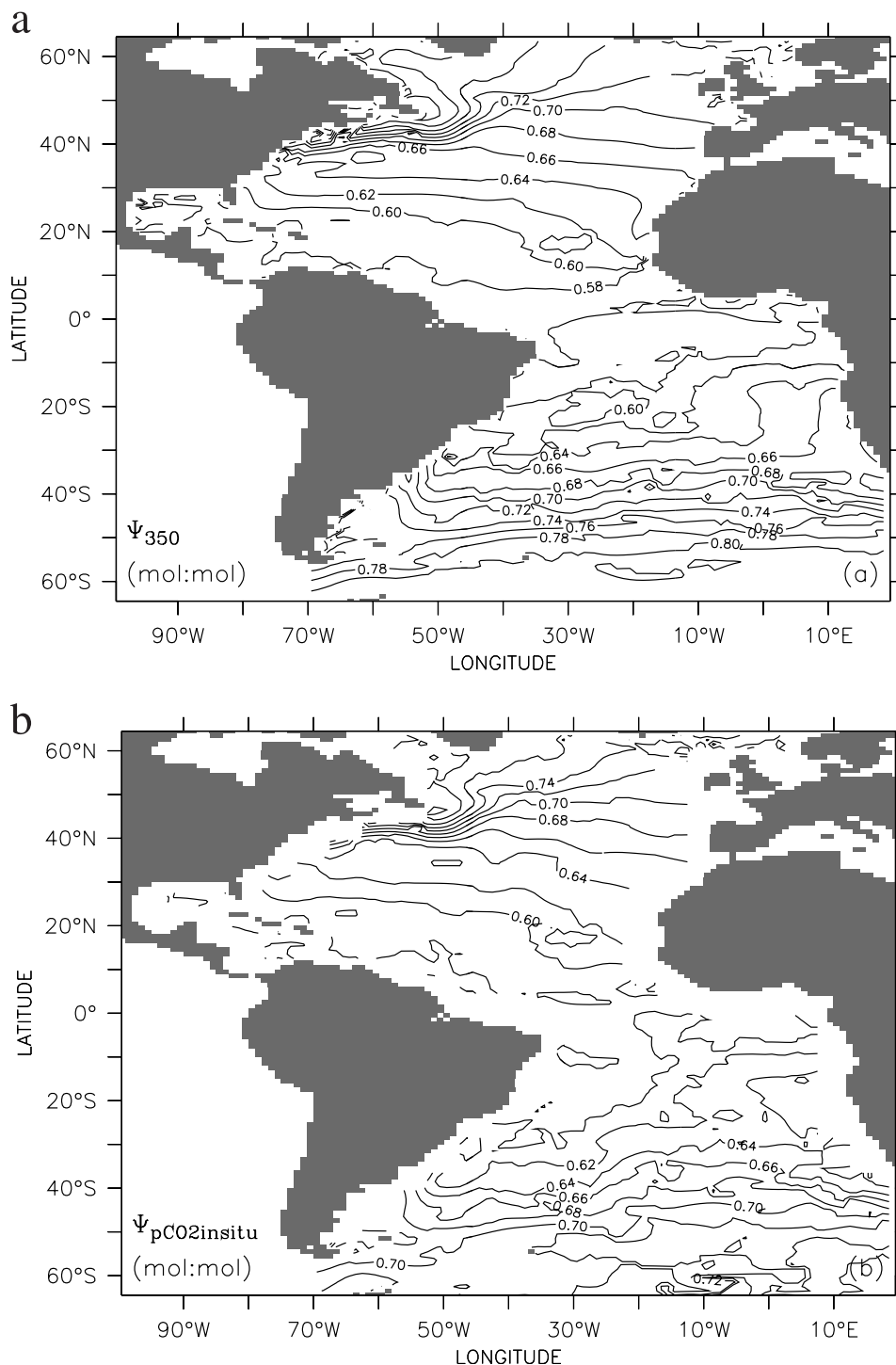
Figure 6. Regional distribution of ψ, the integral ratio of released CO_2:precipitated carbonate during $CaCO_3$ sequestration in the Atlantic Ocean. (a) A pCO_2 of 350 μatm is assumed and ψ is calculated from the relationship $\psi_{350} = 0.8 - 8.3 \times 10^{-3} \times T$ [*Frankignoulle et al.*, 1994] where T is the mixed layer temperature during the time of deepest mixing. Temperature data for this computation where taken from the monthly resolving analyzed temperature ($1° \times 1°$) data set of the WOA98 [*Antonov et al.*, 1998]. The time of deepest mixing was estimated from the climatology of mixed layer depths ($\Delta\sigma = 0.125$ kg m^{-3}) taken from the World Ocean Atlas 1994 (*Monterey and Levitus* [1997]). (b) $\psi_{pCO_2\text{insitu}}$ is ψ at in situ pCO_2 at the time of deepest mixing, $pCO_{2(w)}$. $pCO_{2(w)}$ is taken from Koeve (unpublished data, 2001), basically it is calculated from a sea-air CO_2 difference climatology [*Takahashi et al.*, 1995, 1999] and an estimate of the atmospheric pCO_2 at the time of mixing. The relationship between $\psi_{pCO_2\text{insitu}}$ and ψ_{350} for a given temperature is estimated from a logarithmic fit of data presented in the study by *Frankignoulle et al.* [1994].

4.4. Distribution of J_{eff}

[43] The effective carbon flux, J_{eff}, is calculated according to equation (4) from estimates of $JPOC_{sequ}$ (Figure 4c), $JPIC_{sequ}$, and $\overline{\Psi}$. Several cases are considered. For the standard case (Figure 7a, b) a constant value for $\overline{\Psi}$ of 0.67 is combined with a $JPIC_{sequ}$ data set (Figure 5c) which is computed by applying the POC:PIC ratio estimates from the exponential RR-Z fit, i.e., with one, regionally invariable, vertical distribution of RR. Sensitivity computations are carried out by applying estimates of ψ shown in Figures 6a and b and a depth and regionally variable set of RR, which is computed from RR_{125} shown in Figure 2 and the z-exponent ($e = -0.56$) of the exponential RR-Z function. Throughout this section I will distinguish between estimates for which the calculation of the organic fraction ($JPOC_{sequ}$) is driven by primary production estimates derived by *Antoine et al.* [1996] (AM96 based estimates) and those by *Behrenfeld and Falkowski* [1997] (BF97 based estimates).

[44] Estimates of the basin scale integral of J_{eff} (Table 5) vary between 0.64 and 2.2 GT C m^{-2} yr^{-1}, where the higher estimates are based on the AM96 primary production data set and the lower are based on BF97 primary production data. Most of this difference is due to high AM96-based fluxes in tropical and subtropical waters (Figure 7a, b). Elevated tropical and subtropical AM96 based fluxes are a consistent feature which J_{eff} shares with the distribution of primary production itself, $JPOC_{125}$ (Figure 4a), $JPOC_{sequ}$ (Figure 4c), and $JPIC_{sequ}$ (Figure 5c). On the contrary BF97 based estimates of J_{eff}, in particular the province mean values (Figure 7b), show little structure along the N-S axes. Maxima in temperate and subpolar waters in both hemispheres, which are evident for the export production ($JPOC_{125}$, Figure 4a), have disappeared in the distribution of J_{eff}. The major process that drives this change in the regional distribution is the shallow remineralization of organic carbon.

[45] The fraction of organic carbon export, which is compensated by the CaCO$_3$ sequestration flux ($r_{CaCO_3} = \psi \times JPIC_{sequ}/JPOC_{125}$) is almost constant everywhere in the Atlantic (Figure 7c). For the standard case a slight reduction can be seen in high latitudes of the North Atlantic due to the effect of shallow PIC dissolution (Figure 5b) in waters with deep winter mixing (Figure 4d). The fraction r_{CaCO_3} is more variable if ψ and RR_{exp} are allowed to vary regionally (Figure 7d). The main feature here is a stronger gradient from tropical waters toward mid latitudes and from mid latitudes toward high latitudes in the North Atlantic. r_{CaCO_3} can be up to 50% larger, like in NAST, compared with the standard case. The basin scale effect of regionally variable values of ψ and RR_{exp}, however, is small (Table 5). This is mainly due to the fact that the basin scale averages of the data fields of RR_{exp} (4.15) and ψ ($\psi_{350} = 0.66$ and $\psi_{pCO_2insitu} = 0.64$) are close to the a priori chosen (or from particle flux data estimated) mean values used in the standard case ($\overline{\Psi} = 0.67$; $RR_{exp} = 4.37$). In addition, poleward trends obvious for ψ_{350} or $\psi_{pCO_2insitu}$ and RR_{exp} or RR_{sequ} counteract each other and become insignificant on the basin scale. The use of constant values for ψ and RR_{exp} for the basin-scale estimates of J_{eff} is justified by these findings.

[46] On the basin scale shallow remineralization accounts for $11-17\%$ and CaCO$_3$ compensation for $14-15\%$ of
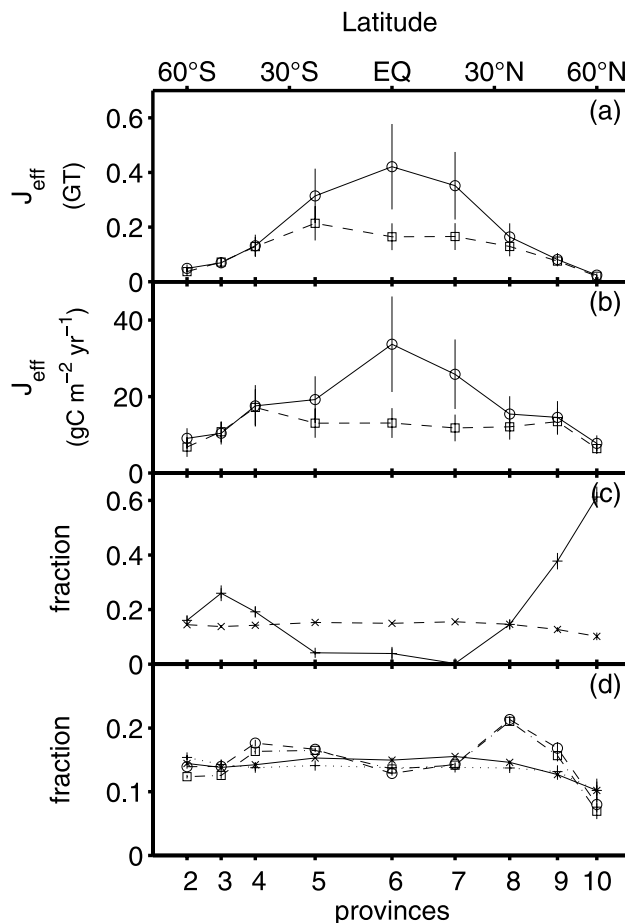

Figure 7. North-south distribution of the effective carbon flux in the Atlantic Ocean. (a-c) Results from the standard case computation (see text). (a) Province integrated J_{eff} (GT carbon yr^{-1}). (b) Province means of J_{eff} (g C m^{-2} yr^{-1}). Solid lines/circles: estimates based on primary production forcing data from the work of *Antoine et al.* [1996], dashed lines/squares: Estimates based on the work of *Behrenfeld and Falkowski* [1997]. (c) Processes which adjust the difference between $JPOC_{125}$ and J_{eff}: solid line (with plus signs) respiration ratio $r_{R-POCsequ} = (JPOC_{125} - JPOC_{sequ})/JPOC_{125}$; dashed line (with asterisks) CaCO$_3$ compensation ratio $\psi \times JPIC_{sequ}/JPOC_{125}$. (d) Regional variation of the CaCO$_3$ compensation ratio for different cases: solid line (x) standard case; dashed line (circles) with RR_{exp} from Figure 2 and ψ from Figure 6a; dash-dotted line (squares) with RR_{exp} from Figure 2 and ψ from Figure 6b; dotted line (with plus signs) $RR_{exp} = 4.37$ from the standard run and ψ from Figure 6b. For province captions see Figure 4.

export production. Overall $JPOC_{exp}$ overestimates the carbon flux which is effective with respect to surface to deep CO$_2$ gradients by about 30% for the Atlantic as a whole and for up to 80% in the subarctic North Atlantic.

5. Summary and Conclusions

[47] The POC:PIC ratio of particle flux in the Atlantic Ocean can be described by two empirical relationships with

almost identical statistics. It is found that a logarithmic fit of the POC:PIC flux ratio and Z, which was adopted from the work of *Antia et al.* [2001], yields an unprecedented increase of PIC flux in the deep ocean and too low POC:PIC ratios of remineralization at intermediate water depths. An exponential fit of the POC:PIC flux ratio over Z, on the other hand, yielded remineralization POC:PIC ratios and deep PIC fluxes which are consistent with independent estimates from the literature.

[48] The basin-scale mean POC:PIC ratio of export production (RR_{exp}) in the Atlantic as estimated from the exponential fit is 4.37. Seasonal changes of nitrate concentrations and alkalinity from temperate and subarctic waters were used in combination with sediment-trap observations from the BATS to construct a map of RR_{exp} which is independent of the deep particle-flux data used elsewhere in this study. Estimates of RR_{exp} ranged between 2 and 9, but the basin-scale integrated value (4.2) agreed with the estimate inferred from deep traps (4.37).

[49] A ratio of organic carbon:inorganic carbon net production, which comprises POC and DOC production, of 6.1–6.9 was recently estimated for the Atlantic by *Lee* [2001] from an analysis of the seasonal changes of total CO_2, alkalinity, and nitrate. The global estimate of the organic carbon:inorganic carbon production ratio of 8.3–9.8 found by *Lee* [2001], which is close to the range of 10–12.5 suggested from a modeling study by *Yamanaka and Tajika* [1996] is particularly due to high values in the subtropical Pacific (13.3–17.4) and the southern ocean (7.0–9.9). These ocean to ocean differences of organic: inorganic uptake ratios between the Atlantic and the Pacific resemble the distinction between a "carbonate ocean" (the Atlantic) and a "silicate ocean" (the Pacific) suggested earlier by *Honjo* [1996].

[50] A map which describes the regional distribution of the vertically and seasonally integrated *released CO_2:precipitated carbonate ratio* (ψ) during $CaCO_3$ formation is prepared for the early 1990s, the time when most of the particle flux studies used in this study where conducted. ψ varies between values around 0.56 in the tropics to values as high as 0.8 in high latitudes, which indicates that $CaCO_3$ sequestration more effectively compensates POC sequestration in high latitudes than in low latitudes. However, the basin scale integral of ψ has about the same value (0.64–0.66) as the first guess choice for a regionally constant ψ (0.67), which was estimated to be consistent with the mean surface ocean pCO_2 equilibration temperature of the contemporary ocean.

[51] Estimates of J_{eff} ranged from 0.66 to 2.18 GT C yr^{-1}, this large range is in particular due to the propagation of regional differences of primary production maps [*Antoine et al.*, 1996; *Behrenfeld and Falkowski*, 1997], which are used as forcing data to estimate the flux of organic carbon in this study. The integrated POC:PIC sequestration flux ratio for the Atlantic ocean is about 3.9, with much lower values in the subarctic North Atlantic. On the basin scale shallow remineralization of POC and $CaCO_3$ compensation are about equally important in adjusting J_{eff}. The effect of $CaCO_3$ compensation on POC sequestration shows little regional variations and no correlation with the depth of winter-time mixing. The importance of shallow respiration
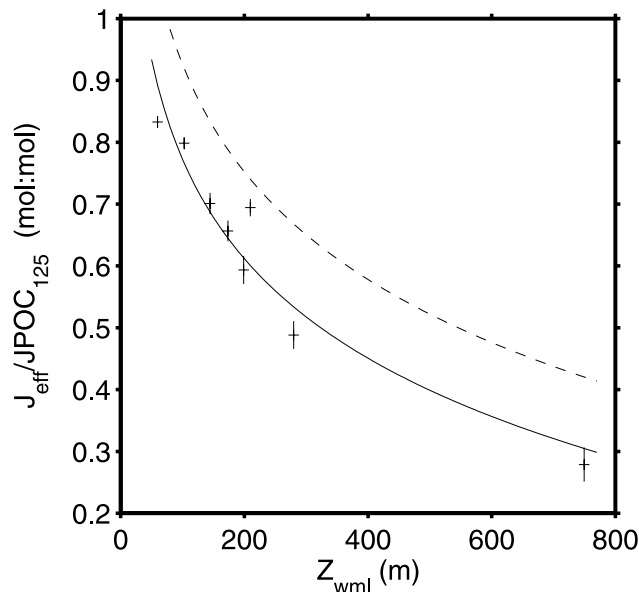

Figure 8. The relation between the province mean of the relative effectivity of the biological pump (eff = J_{eff}/JPOC$_{125}$) and Z_{sequ}. Data points are province means (±s.d.); solid line: logarithmic fit to the data J_{eff}/JPOC$_{125}$ = 1.84 − 0.23 ln(Z); r^2 = 0.925); dashed line: the respective fit for the ratio JPOC$_{sequ}$/JPOC$_{125}$ (JPOC$_{sequ}$/JPOC$_{125}$ = 2.08 − 0.25 ln(Z); r^2 = 0.926). The equatorial province WETRA was excluded from this analysis, since the seasonal variability of the mixed layer depth there is meaningless in the context of this study.

for POC sequestration shows more distinct regional patterns. While in tropical and subtropical waters this process is negligible, up to about 61% of export production is remineralized in high latitude waters in the North Atlantic. The strong link between winter mixed layer depth and the relative effectivity of the biological pump (eff = J_{eff}/JPOC$_{exp}$) is summarized in Figure 8. About 92% of the variation of J_{eff}/JPOC$_{125}$ can be explained by the depth of the winter mixed layer.

[52] With an anticipated change of ocean stratification due to global warming and the intensification of the water cycle [*Manabe et al.*, 1991; *Sarmiento et al.*, 1998], export production likely will change due to reduced nutrient fluxes to the surface ocean and a perhaps prolonged growth season [*Bopp et al.*, 2001]. Much of this change is likely to become compensated by simultaneous changes of CO_2 fluxes into the surface ocean [*Maier-Reimer et al.*, 1996].

[53] The increase in the effectivity of the biological pump (rising J_{eff}/JPOC$_{exp}$, Figure 8), however, constitutes a negative feedback process which can give rise to an imbalance in ocean carbon fluxes on timescales of the response of ocean circulation and thereby can increase the flux of anthropogenic CO_2 flux into the ocean. An example of such a transient imbalance is described in a climate model study by *Joos et al.* [1999]. There the feedback of the biological pump around year 2100 increases the oceanic CO_2-uptake by about 10–15%, and thereby compensates for about 30–40%

of the reduction in CO_2 uptake from the combined effect of changes in the ocean circulation and the surface ocean temperature (i.e., higher ocean pCO_2 due to higher surface ocean temperature and hence a reduced CO_2 uptake). Model predictions of the regional distribution of changes in the mixed layer depth [*Bopp et al.*, 2001] would indicate that temperate and subarctic waters, but not the tropics, will be the sites which show the most significant changes in terms of effective carbon fluxes into the deep ocean.

Appendix A: Estimating the Surface Mixed Layer POC:PIC Ratio of Production From Climatological Data

[54] Operationally it is assumed that the fraction of new carbon production (NP) which is exported via particles can be estimated from the seasonal drawdown of nitrate by multiplying with an appropriate C:N ratio of particles (equation (A1)). A C:N ratio of 6.625 [*Redfield et al.*, 1963; *Körtzinger et al.*, 2001a] is used in this study. The seasonal nitrate drawdown (ΔNO_3) is estimated as the difference between an estimate of the winter nitrate concentration ($NO_{3(w)}$) and the local minimal nitrate concentration ($\min(NO_{3(seasonal)})$) observed in the seasonal nitrate climatology [*NODC World Ocean Atlas*, 1998 (WOA98; *Conkright et al.*, 1998]. The winter nitrate concentration is calculated by applying the integration method of *Glover and Brewer* [1988] to the annual winter nitrate climatology from WOA98 (equation (A2))

$$NP = C/N \times \Delta NO_3 = C/N \times [NO_{3w} - \min(NO_{3(seasonal)})]$$
(A1)

$$NO_{3(W)} = 1/Z_{wml} \times \int_0^{Z_{wml}} NO_{3(annual)}$$
(A2)

[55] The production and export of $CaCO_3$ in the mixed layer, P_{CaCO_3} is estimated analogue to the approach of *Robertson et al.* [1994] from the seasonal change in potential alkalinity (equation (A3)). Here ΔNTA is the seasonal difference of the salinity normalized total alkalinity (NTA). NTA is estimated from regionally variable empirical relationships with temperature [*Millero et al.*, 1998]. Monthly mean temperature values for the calculation of monthly NTA data fields are taken from WOA98 [*Antonov et al.*, 1998]

$$P_{CaCO_3} = [\Delta NTA + \Delta NO_3]/2$$
(A3)

[56] Thereafter the mixed layer POC:PIC ratio of production, $RR_{mixed-layer}$, is estimated as the ratio of NP/P_{CaCO_3}.

[57] In the subtropics and tropics the seasonal approach cannot be used since seasonal gradients of alkalinity and nitrate vanish. As a substitute for the subtropical bands ($10°-35°N$, $10°-35°S$) I estimate RR_{exp} from mass flux and organic carbon flux data from drifting particle interceptor trap measurements (150 m depth) at the BATS [*Lohrenz et al.*, 1992]. Since particle flux measurements at BATS do not include measurements of $CaCO_3$ fluxes,

RR_{exp} is calculated assuming that the dry weight mass flux consists of organic matter (2.3POC), $CaCO_3$, opal, and a residual terrigenous component [*Jickells et al.*, 1998], and that the opal to $CaCO_3$ ratio and the fraction of terrigenous matter can be extrapolated from deep trap observations from the close-by OFP-site. The long-term mean of the fraction of terrigenous matter in 3200 m at the OFP-site close to BATS is 18.7% [*Conte et al.*, 2001] and the opal to $CaCO_3$ weight ratio during the early 1990s was 0.18 [*Deuser et al.*, 1995]. Using the z-exponent of organic carbon flux decreases with depth from Koeve (submitted manuscript, 2001), the z-exponent of the $CaCO_3$ exponential flux function (this study) and a temperature dependent decay rate of opal [*Gnanadesikan*, 1999], a mean terrigenous fraction, and a mean $[opal/CaCO_3]_{weight}$ ratio in 150 m of 3% and 0.26, respectively, are estimated. Mass dry weight and POC data (available from the home page of the BATS Program at http://www.bbsr.edu) from traps deployed at 150 m between December 1988 and December 1997 ($n = 106$) are used. The median POC:PIC ratio in 150 m at BATS calculated from these data is 4.5, the time integrated annual mean POC:PIC ratio is 4.1. The latter value is used as an estimate of RR_{exp} in the subtropical band ($10°-35°$); in the tropics ($10°S-10°N$) an export flux ratio of 4.37 is used (Figure 2).

References

Antia, A. N., et al., Basin-wide particulate carbon flux in the Atlantic Ocean: Regional export patterns and potential for atmospheric carbon sequestration, *Global Biogeochem. Cycles*, 15, 845–862, 2001.

Antoine, D., and A. Morel, Oceanic primary production, 1, Adaptation of a spectral light-photosynthesis model in view of application to satellite chlorophyll observations, *Global Biogeochem. Cycles*, 10, 43–55, 1996.

Antoine, D., J.-M. André, and A. Morel, Oceanic primary production, 2, Estimation at global scale from satellite (coastal zone color scanner) chlorophyll, *Global Biogeochem. Cycles*, 10, 57–69, 1996.

Antonov, J., S. Levitus, T. P. Boyer, M. Conkright, T. O'Brien, and C .Stephens, *World Ocean Atlas 1998*, vol. 1, *Temperature of the Atlantic Ocean. NOAA Atlas NESDIS 27*, p. 166, U.S. Government Printing Office, Washington, D.C., 1998.

Archer, D., Modelling the calcite lysocline, *J. Geophys. Res.*, 96C, 17,037–17,050, 1991.

Archer, D., A data-driven model of the global calcite lysocline, *Global Biogeochem. Cycles*, 10, 511–526, 1996.

Archer, D., A. Winguth, D. Lea, and N. Mahowald, What caused the glacial/interglacial atmospheric CO_2 cycles?, *Rev. Geophys.*, 38, 159–189, 2000a.

Archer, D. A., G. Eshel, A. Winguth, W. Broecker, R. Pierrehumbert, and M. Tobis, Atmospheric pCO_2 sensitivity to the biological pump in the ocean, *Global Biogeochem.*, 1219–1230, 2000b.

Asper, V. L., Particle flux in the ocean: Oceanographic tools, in *Particle Flux in the Ocean*, edited by V. Ittekkot et al., pp. 71–84, John Wiley, New York, 1996.

Bacastow, R., and E. Maier-Reimer, Ocean-circulation model of the carbon cycle, *Clim. Dyn.*, 4, 95–125, 1990.

Balch, W. M., K. A. Kilpatrick, P. Holligan, D. Harbour, and E. Fernandez, The 1991 coccolithophore bloom in the central North Atlantic, 2 Relating

optics to coccolith concentration, *Limnol. Oceanogr.*, *41*, 1684–1696, 1996.

Behrenfeld, M. J., and P. G. Falkowski, Photosynthetic rates derived from satellite-based chlorophyll concentrations, *Limnol. Oceanogr.*, *42*, 1–20, 1997.

Berger, W. H., Global maps of ocean productivity, in *Productivity of the Ocean: Present and Past*, edited by W. H. Berger, V. S. Smetacek, and G. Wefer, pp. 429–455, John Wiley, New York, 1989.

Berger, W. H., K. Fisher, C. Lai, and G. Wu, Oceanic productivity and organic carbon flux, *Scr. Inst. Ocean. Ref.*, *87–30*, 1–67, 1987.

Betzer, P. R., W. J. Showers, E. A. Laws, C. D. Winn, G. R. DiTullio, and P. M. Kroopnick, Primary productivity and particle fluxes on a transect of the equator at 153°W in the Pacific Ocean, *Deep Sea Res.*, *31*, 1–11, 1984.

Bopp, L., P. Monfray, O. Aumont, J.-L. Dufresne, H. Le Treut, G. Madec, L. Terray, and J. C. Orr, Potential impact of climate change on marine export production, *Global Biogeochem. Cycles*, *15*, 81–99, 2001.

Broecker, W. S., and T.-H. Peng, *Tracers in the Sea*, p. 690, Columbia Univ. Press, New York, 1982.

Brzezinski, M. A., The Si:C:N ratio of marine diatoms: Interspecific variability and the effect of some environmental variables, *J. Phycol.*, *21*, 347–357, 1985.

Brzezinski, M. A., A. L. Alldredge, and L. M. O'Bryan, Silica cycling within marine snow, *Limnol. Oceanogr.*, *42*, 1706–1713, 1997.

Buesseler, K. O., Do upper-ocean sediment traps provide an accurate record of particle flux?, *Nature*, *353*, 420–423, 1991.

Buitenhuis, E. T., P. van der Wal, and H. J. W. de Baar, Blooms of *Emiliania huxleyi* are sinks of atmospheric carbon dioxide: A field and mesocosm study derived simulation, *Global Biogeochem. Cycles*, *15*, 577–588, 2001.

Carlson, C. A., H. W. Ducklow, and A. F. Michaels, Annual flux of dissolved organic carbon from the euphotic zone in the northwestern Sargasso Sea, *Nature*, *371*, 405–408, 1994.

Conkright, M., T. O'Brien, S. Levitus, T. P. Boyer, J. Antonov, and C. Stephens, *World Ocean Atlas 1998*, vol. 10, *Nutrients and Chlorophyll of the Atlantic Ocean. NOAA Atlas NESDIS 36*, p. 245, U.S. Govt. Print. Off., Washington, D.C., 1998.

Conte, M. H., N. Ralph, and E. H. Ross, Seasonal and interannual variability in deep ocean particle flux at the Oceanic Flux Program (OFP)/Bermuda Atlantic Time Series (BATS) site in the western Sargasso Sea near Bermuda, *Deep Sea Res., Part II*, *48*, 1471–1505, 2001.

Deuser, W. G., T. D. Jickells, P. King, and J. A. Commeau, Decadal and annual changes in biogenic opal and carbonate fluxes to the deep Sargasso Sea, *Deep Sea Res., Part*, *42*, 1923–1933, 1995.

Doval, M. D., and D. A. Hansell, Organic carbon and apparent oxygen utilization in the western South Pacific and the central Indian Ocean, *Mar. Chem.*, *68*, 249–264, 2000.

Eppley, R. W., and B. J. Peterson, Particulate organic matter flux and planktonic new production in the deep ocean, *Nature*, *282*, 677–680, 1979.

Fasham, M. J. R., B. M. Balino, and M. C. Bowles, A new vision of ocean biogeochemistry after a decade of the Joint Global Ocean Flux Study (JGOFS), *Ambio Spec. Rep.*, *10*, 4–30, 2001.

Fernandez, E., P. Boyd, P. M. Nolligan, and D. S. Harbour, Production of organic and inorganic carbon within a large-scale coccolithophore bloom in the northeast Atlantic Ocean, *Mar. Ecol. Prog. Ser.*, *97*, 271–285, 1993.

Fiadeiro, M., The alkalinity of the deep pacific, *Earth Planet Sci. Lett.*, *49*, 499–505, 1980.

Fowler, S. W., and G. A. Knauer, Role of large particles in the transport of elements and organic compounds through the oceanic water column, *Prog. Oceanogr.*, *16*, 147–194, 1986.

Frankignoulle, M., C. Canon, and J.-P. Gattuso, Marine calcification as a source of carbon dioxide: Positive feedback of increasing atmospheric CO_2, *Limnol. Oceanogr.*, *39*, 458–462, 1994.

Glover, D. M., and P. G. Brewer, Estimates of wintertime mixed layer nutrient concentration in the North Atlantic, *Deep Sea Res.*, *35*, 1525–1546, 1988.

Gnanadesikan, A., A global model of silicon cycling: Sensitivity to eddy parameterization and dissolution, *Global Biogeochem. Cycles*, *13*, 199–220, 1999.

Gust, G., B. R. E. Byrne, P. R. Betzer, and W. Bowles, Particle fluxes and moving fluids: Experience from synchronous trap collections in the Sargasso Sea, *Deep Sea Res.*, *39*, 1071–1083, 1992.

Hargrave, B. T., Particle sedimentation in the ocean, *Ecol. Modell.*, *30*, 229–246, 1985.

Harris, R. P., Zooplankton grazing on the coccolithophore *Emiliania huxleyi* and its role in inorganic carbon, *Mar. Biol.*, *119*, 431–439, 1994.

Holligan, P. M., and W. M. Balch, From the ocean to cells: Coccolithophore optic and biogeochemistry, in Particle Analysis in Oceanography, NATO ASI Ser., vol. G 27, edited by S. Demers, pp. 301–324, Springer-Verlag, New York, 1991.

Holligan, P. M., et al., A biogeochemical study of the coccolithophore, *Emiliania huxleyi*, in the North Atlantic, *Global Biogeochem. Cycles*, *7*, 879–900, 1993.

Honjo, S., Particle fluxes and modern sedimentation in the Polar Oceans, in *Polar Oceanography, Part B*, edited by W. O. J. Smith, Academic San Diego, Calif., pp. 687–739, 1990.

Honjo, S., Fluxes of particles to the interior of the open ocean, in *Particle Flux in the Ocean*, edited by V. Ittekkot et al., pp. 91–154, 1996.

Honjo, S., and S. J. Manganini, Annual biogenic particle fluxes to the interior of the North Atlantic Ocean; studied at 34°N 21°W and 48°N 21°W, *Deep Sea Res., Part II*, *40*, 587–608, 1993.

Honjo, S., and M. R. Roman, Marine copepod fecal pellets: Production, transportation and sedimentation, *J. Mar. Res.*, *36*, 45–57, 1978.

Jickells, T. D., S. Dorling, W. G. Deuser, T. M. Church, R. Arimoto, and J. M. Prospero, Air-borne dust to a deep water sediment trap in the Sargasso Sea, *Global Biogeochem. Cycles*, *12*, 311–320, 1998.

Joos, F., G.-K. Plattner, T. F. Stocker, O. Marchal, and A. Schmittner, Global warming and marine carbon cycle feedbacks on future atmospheric CO_2, *Science*, *284*, 464–467, 1999.

Kähler, P., and E. Bauerfeind, Organic particles in a shallow sediment trap: Substantial loss to the dissolved phase, *Limnol. Oceanogr.*, *46*, 719–723, 2001.

Kähler, P., and W. Koeve, Marine dissolved organic matter: Can its C/N ratio explain carbon overconsumption?, *Deep Sea Res., Part I*, *48*, 49–62, 2001.

Keir, R. S., The dissolution kinetics of biogenic calcium carbonates in seawater, *Geochim. Cosmochim. Acta*, *44*, 241–252, 1980.

Koeve, W., Wintertime nutrients in the North Atlantic – New approaches and implications for estimates of seasonal new production, *Mar. Chem.*, *74*, 245–260, 2001.

Körtzinger, A., W. Koeve, P. Kähler, and L. Mintrop, C:N ratios in the mixed layer during the productive season in the northeast Atlantic ocean, *Deep Sea Res., Part I*, *48*, 661–688, 2001a.

Körtzinger, A., J. I. Hedges, and P. D. Quay, Redfield ratios revisited—Removing the biasing effect of anthropogenic CO2, *Limnol. Oceanogr.*, *46*, 964–970, 2001b.

Lee, K., Global net community production estimated from the annual cycle of surface water total dissolved inorganic carbon, *Limnol. Oceanogr.*, *46*, 1287–1297, 2001.

Li, Y.-H., T. Takahashi, and W. S. Broecker, Degree of saturation of $CaCO_3$ in the oceans, *J. Geophys. Res.*, *74*, 5507–5525, 1969.

Lohrenz, S. E., G. A. Knauer, V. L. Asper, M. Tuel, A. F. Michaels, and A. H. Knap, Seasonal variability in primary production and particle flux in the northwestern Sargasso Sea: U.S. JGOFS Bermuda Atlantic Time-series Study, *Deep Sea Res.*, *39*, 1373–1391, 1992.

Longhurst, A., Ecological geography of the sea, p. 398, Academic, San Diego, Calif., 1998.

Longhurst, A., S. Sathyendranath, T. Platt, and C. Caverhill, An estimate of global primary production in the ocean from satellite radiometer data, *J. Plankton Res.*, *17*, 1245–1271, 1995.

Louanchi, F., and R. G. Najjar, A global monthly climatology of phosphate, nitrate and silicate in the upper ocean: Spring-summer export production and shallow remineralization, *Global Biogeochem. Cycles*, *14*, 957–977, 2000.

Maier-Reimer, E., U. Mikolajewicz, and A. Winguth, Future ocean uptake of CO_2: Interaction between ocean circulation and biology, *Clim. Dyn.*, *12*, 711–721, 1996.

Manabe, S., R. J. Stouffer, M. J. Spelman, and K. Bryan, Transient response of a coupled ocean-atmosphere model to gradual changes of atmospheric CO_2 I, annual mean response, *J. Clim.*, *4*, 785–818, 1991.

Martin, J. H., G. A. Knauer, D. M. Karl, and W. W. Broenkow, VERTEX: Carbon cycling in the northeast Pacific, *Deep Sea Res.*, *34*, 267–285, 1987.

Martin, J. H., S. E. Fitzwater, R. M. Gordon, C. N. Hunter, and S. J. Tanner, Iron, primary production and carbon-nitrogen flux studies during the JGOFS North Atlantic Bloom Experiment, *Deep Sea Res., Part II*, *40*, 115–134, 1993.

Michaels, A. F., M. W. Silver, M. M. Gowing, and G. A. Knauer, Cryptic zooplankton swimmers in upper ocean sediment traps, *Deep Sea Res.*, *37*, 1285–1296, 1990.

Millero, F. J., K. Lee, and M. Roche, Distribution of alkalinity in the surface waters of the major oceans, *Mar. Chem.*, *60*, 111–130, 1998.

Milliman, J. D., Production and accumulation of calcium carbonate in the ocean: Budget of a non steady state, *Global Biogeochem. Cycles*, *7*, 927–957, 1993.

Milliman, J. D., P. J. Troy, W. M. Balch, A. K. Adams, Y.-H. Li, and F. T. Mackenzie, Biologically mediated dissolution of calcium carbonate above the chemical lysocline?, *Deep Sea Res., Part I*, *46*, 1653–1669, 1999.

Monterey, G., and S. Levitus, *Seasonal Variability of Mixed Layer Depth for the World Ocean. NOAA Atlas NESDIS 14*, p. 96, U.S. Govt. Print. Off., Washington, D.C., 1997.

Najjar, R. G., J. L. Sarmiento, and J. R. Toggweiler, Downward transport and fate of organic matter in the ocean: Simulations with a general circulation model, *Global Biogeochem. Cycles*, *6*, 45–76, 1992.

Oschlies, A., W. Koeve, and V. Garçon, An eddy-permitting coupled physical-biological model of the North Atlantic, II, Ecosystem dynamics and comparison with satellite and JGOFS local studies data, *Global Biogeochem. Cycles*, *14*, 499–523, 2000.

Pace, M. L., G. A. Knauer, D. M. Karl, and J. H. Martin, Primary production, new production and vertical flux in the eastern Pacific Ocean, *Nature*, *325*, 803–804, 1987.

Peterson, M. N. A., Calcite: Rates of dissolution in a vertical profile in the Central Pacific, *Science*, *54*, 1542–1544, 1966.

Ploug, H., and B. B. Jørgensen, A net-jet flow system for mass transfer and microsensor studies of sinking aggregates, *Mar. Ecol. Prog. Ser.*, *176*, 279–290, 1999.

Pomeroy, L. R., and R. E. Johannes, Occurrence and respiration of ultraplankton in the upper 500 m of the ocean, *Deep Sea Res.*, *15*, 381–391, 1968.

Pond, D. W., R. P. Harris, and C. A. Brownlee, Microinjection technique using a pH-sensitive dye to determine the gut pH of Calanus helgolandicus, *Mar. Biol.*, *123*, 75–79, 1995.

Redfield, A. C., B. H. Ketchum, and F. A. Richards, The influence of organisms on the composition of seawater, in *The Sea*, vol. 2, edited by M. N. Hill, pp. 26–77, John Wiley, New York, 1963.

Richards, F. A., Dissolved silicate and related properties of some western North Atlantic and Caribbean waters, *J. Mar. Res.*, *17*, 449–465, 1958.

Riebesell, U. Z. I., B. Rost, P. D. Tortell, R. E. Zeebe, and F. M. M. Morel, Reduced calcification of marine plankton in response to increased atmospheric CO_2, *Nature*, *407*, 364–367, 2000.

Riley, G. A., Organic aggregates in seawater and the dynamics of their formation and utilization, *Limnol. Oceanogr.*, *8*, 265–279, 1963.

Robertson, J. E., C. Robinson, D. R. Turner, P. Holligan, A. J. Watson, P. Boyd, E. Fernandez, and M. Finch, The impact of a coccolithophore bloom on oceanic carbon uptake in the northeast Atlantic during summer 1991, *Deep Sea Res., Part I*, *41*, 297–314, 1994.

Sambrotto, R. N., J. H. Martin, W. W. Broenkow, C. Carlson, and S. E. Fitzwater, Nitrate utilization in surface waters of the Iceland Basin during spring and summer of 1989, *Deep-Sea Res., Part II*, *40*, 441–458, 1993.

Sarmiento, J. L., R. D. Slater, M. J. R. Fasham, H. W. Ducklow, J. R. Toggweiler, and G. T. Evans, A seasonal three-dimensional ecosystem model of nitrogen cycling in the North Atlantic euphotic zone, *Global Biogeochem. Cycles*, *7*, 417–450, 1993.

Sarmiento, J. L., T. M. C. Hughes, R. J. Stouffer, and S. Manabe, Simulated response of the ocean carbon cycle to anthropogenic climate warming, *Nature*, *393*, 245–249, 1998.

Scholten, J. C., J. Fietzke, S. Vogler, M. Rutgers van der Loeff, A. Mangini, W. Koeve, J. Waniek, P. Stoffers, A. Antia, and J. Kuss, Trapping efficiency of sediment traps from the deep eastern North Atlantic: The [230]Th calibration, *Deep Sea Res., Part II*, *48*, 2383–2408, 2001.

SCOR, *The Joint Global Ocean Flux Study – JGOFS- Science Plan*, 61 pp., Scientific Committee on Oceanic Research, International Council of Scientific Unions, Halifax, 1990.

Shaffer, G., Effects of the marine biota on global carbon cycling, in *The Global Carbon Cycle*, edited by M. Heimann, pp. 431–455, Springer-Verlag, New York, 1993.

Sigman, D. M., D. C. McCorkle, and W. R. Martin, The calcite lysocline as a constraint on glacial/interglacial low-latitude production changes, *Global Biogeochem. Cycles*, *12*, 409–427, 1998.

Six, K. D., and E. Maier-Reimer, Effects of plankton dynamics on seasonal carbon fluxes in an ocean general circulation model, *Global Biogeochem. Cycles*, *10*, 559–583, 1996.

Sokal, R. R., and F. J. Rohlf, Biometry – The principles and practice of statistics in biological research, 3rd ed., 887 pp., W. H. Freeman, New York, 1995.

Suess, E., Particulate organic carbon flux in the ocean–Surface productivity and oxygen utilization, *Nature*, *288*, 260–263, 1980.

Takahashi, T., Carbonate chemistry of seawater and the calcite compensation depth in the oceans Spec. Publ. Cushman Found, *Foramin. Res.*, *13*, 11–126, 1975.

Takahashi, T., W. S. Broecker, and S. Langer, Redfield ratio based on chemical data from isopycnal surfaces, *J. Geophys. Res.*, *90c*, 6907–6924, 1985.

Takahashi, T., T. T. Takahashi, and S. C. Sutherland, An assessment of the role of the North Atlantic as a CO_2 sink, *Philos. Trans.R. Soc. London, Ser. B*, *348*, 143–152, 1995.

Takahashi, T., R. H. Wanninkhof, R.A. Feely, R.F. Weiss, D. W. Chipman, N. Bates, J. Olafsson, C. Sabine, and S. C. Sutherland, Net sea-air CO_2 flux over the global oceans: An improved estimate based on the sea-air pCO_2 difference, *Proceedings of the 2nd International Symposium CO_2 in the Oceans, Tsukuba, January 1999, CGER-1037-'99, CGER/NIES*, pp. 9–15, 1999.

Tsungogai, S., and S. Noriki, Particle fluxes of carbonate and organic carbon in the ocean. Is the marine biological activity working as a sink of the atmospheric carbon?, *Tellus, Ser. B*, *43*, 256–266, 1991.

Turley, C. M., Formation, vertical flux and remineralisation of aggregates in the ocean: A short review, *Arch. Hydrobiol. Beih.*, *37*, 155–163, 1992.

Veldhuis, M. J. W., G. W. Kraay, and W. W. C. Gieskes, Growth and fluorescence characteristics of ultraplankton on a north-south transect in the eastern North Atlantic, *Deep Sea Res., Part II*, *40*, 609–626, 1993.

Volk, T., and M. I. Hoffert, Ocean carbon pumps, analysis of relative strengths and efficiencies in ocean-driven atmosphere CO_2 changes, in *The Carbon Cycle and Atmospheric CO_2: Natural Variations Archean to Present*, edited by E. T. Sundquist and W. S. Broecker, pp. 99–110, *Geophys. Monogr.*, AGU, Washington, D.C., *32*, 1985.

Ware, J. R., S. V. Smith, and M. L. Reaka-Kudla, Coral reefs: Sources or sinks of atmospheric CO_2?, *Coral Reefs*, *11*, 127–130, 1992.

Yamanaka, Y., and E. Tajika, The role of the vertical fluxes of particulate organic matter and calcite in the oceanic carbon cycle: Studies using an ocean biogeochemical general circulation model, *Global Biogeochem. Cycles*, *10*, 361–382, 1996.

Zeitzschel, B., P. Diekmann, and L. Uhlmann, A new multisample sediment trap, *Mar. Biol.*, *45*, 285–288, 1978.

Zondervan, I., R. E. Zeebe, B. Rost, and U. Riebesell, Decreasing marine biogenic calcification: A negative feedback on rising atmospheric pCO_2, *Global Biogeochem. Cycles*, *15*, 507–516, 2001.

———————————
W. Koeve, Zentrum für marine Umweltwissenschaften, (Marum), Fachbereich Geowissenschaften (FB5), Universität Bremen, Postfach 330440, D-28334 Bremen, Germany. (w.koeve@web.de; w.koeve@surfeu.de)